CAPITAL UNIVERSITY OF SCIENCE AND
TECHNOLOGY, ISLAMABAD

Validation of Pathloss Models Through Field Measurements

by

Sunbal Iftikhar

A thesis submitted in partial fulfillment for the
degree of Master of Science

in the

Faculty of Engineering
Department of Electrical Engineering

2020

I dedicate this work to my dearest parents for their affectionate love, support and encouragement.

CERTIFICATE OF APPROVAL

Validation of Pathloss Models Through Field Measurements

by

Sunbal Iftikhar

(MEE173012)

THESIS EXAMINING COMMITTEE

S. No.	Examiner	Name	Organization
(a)	External Examiner	Dr. Zia ul Haq Abbas	GIKI, Peshawar
(b)	Internal Examiner	Dr. Tahir Awan	CUST, Islamabad
(c)	Supervisor	Dr. Noor Muhammad Khan	CUST, Islamabad

Dr. Noor Muhammad Khan
Thesis Supervisor
February, 2020

Dr. Noor Muhammad Khan
Head
Dept. of Electrical Engineering
February, 2020

Dr. Imtiaz Ahmad Taj
Dean
Faculty of Engineering
February, 2020

Author's Declaration

I, **Sunbal Iftikhar** hereby state that my MS thesis titled "**Validation of Pathloss Models Through Field Measurements**" is my own work and has not been submitted previously by me for taking any degree from Capital University of Science and Technology, Islamabad or anywhere else in the country/abroad.

At any time if my statement is found to be incorrect even after my graduation, the University has the right to withdraw my MS Degree.

(Sunbal Iftikhar)
Registration No: MEE173012

Plagiarism Undertaking

I solemnly declare that research work presented in this thesis titled "**Validation of Pathloss Models Through Field Measurements**" is solely my research work with no significant contribution from any other person. Small contribution/help wherever taken has been dully acknowledged and that complete thesis has been written by me.

I understand the zero tolerance policy of the HEC and Capital University of Science and Technology towards plagiarism. Therefore, I as an author of the above titled thesis declare that no portion of my thesis has been plagiarized and any material used as reference is properly referred/cited.

I undertake that if I am found guilty of any formal plagiarism in the above titled thesis even after award of MS Degree, the University reserves the right to withdraw/revoke my MS degree and that HEC and the University have the right to publish my name on the HEC/University website on which names of students are placed who submitted plagiarized work.

(Sunbal Iftikhar)
Registration No: MEE173012

Acknowledgements

After being utmost grateful to Allah Almighty who gave me help and courage to complete my M.S thesis, I would like to express huge gratitude to my supervisor **Dr. Noor Muhammad Khan** whose continuous support, guidance, and rightful critics kept me steering in the right direction throughout my research work. I am fortunate to work with him which made me able to benefit myself from his knowledge regarding research skills and wireless communication systems.

I would also like to express my thanks to my dearest parents; my Father Raja Iftikhar Ahmed, and my Mother Azra Iftikhar who always supported me during thick and thin and encouraged me to stay motivated throughout my degree program in order to achieve my goals.

(Sunbal Ifikhar)

Registration No: MEE173012

Abstract

A propagation pathloss model (PLM) is an important tool in wireless network planning that allows network planners to optimize the cell towers' distribution and meet expected service level requirements. In this thesis, different PLMs (Hata-Okumura, ECC-33, Ericson, SUI, Lognormal shadowing, and COST-231) have been analyzed and compared with field measurement data. Field measurements are carried out on Islamabad Expressway, Pakistan receiving signals from the base stations (BTSs) located at Koral Town (BTS1), Korang Town (BTS2), and Soan Garden (BTS3). Upon comparison, results show that the Lognormal shadowing PLM showed the closest agreement to the measured pathloss with a minimum error of 2.86% and 2.17% for BTS1 and BTS2 respectively. The measured pathloss in BTS3 is best estimated by the Hata-Okumura PLM with an error of 9.59%.

In wireless networks, theoretical PLMs are largely based on single slope PLM, which falls short in accurately capturing the fading effects of the physical propagation environment. However, the analysis of the measurement data does not show agreement with this practice and reflects a multi-slope behavior. The impact of the multi-slope phenomenon is evident from the variation in the pathloss exponents of different segments of Islamabad Expressway. The lognormal shadowing PLM is thus chosen based on its smallest error with the measured pathloss data and is further extended to multi-slope lognormal shadowing PLM. It is observed that the proposed multi-slope lognormal shadowing PLM leads to an improvement of 24.8% in its agreement with measurement data reducing the minimum error to 2.15% for BTS1.

Contents

List of Figures

List of Tables

Abbreviations

BTS	Base Station
BTS1	Base Station1
BTS2	Base Station2
BTS3	Base Station3
COST	European Cooperation in Science and Technology
CCIR	International Radio Consultative Committee
dB	decibel
dBm	decibel milliwatts
ECC	Electronics Communication Committee
EIRP	Effective Isotropically Radiated Power
FWA	Fixed Wireless Access System
GPP	Generation Project Partnership
GA	Genetic Algorithm
GSM	Global System for Mobile
GPS	Global Positioning System
GHz	Giga Hertz
HetNet	Heterogeneous Network
ID	Identity
ITU	International Telecommunication Union
km	Kilometers
Lat	Latitude
Long	Longitute
LTE	Long-Term Evolution
LDPL	Log-distance Pathloss

MTS	Mobile Terminal Station
MMDS	Multipoint Microwave Distribution System
MHz	Mega Hertz
m	Meters
MSE	Mean Square Error
NMEA	National Marine Electronics Association
PLE	Pathloss Exonent
PLM	Pathloss Model
PL	Pathloss
PSO	Particle Swarm Optimization
PDP	Power Delay Profile
RSS	Received Signal Strength
SUI	Standford University Interim
SIR	Signal-to-Interference Ratio
SNR	Signal-to-Noise Ratio
SINR	Signal-to-Interference-plus-Noise Ratio
T-R	Transmitter and Receiver
TEMS	Test Equipment for Mobile System
UTD	Uniform Theory of Diffraction
UMTS	Universal Mobile Telecommunication System
UHF	Ultra High Frequency
V2V	Vehicle to Vehicle
V2I	Vehicle to Infrastructure
WCS	Wireless Communication System
3G	Third Generation
4G	Fourth Generation
3D	Three Dimensional

Symbols

P_{t}	Transmitted Power
G_{t}	Transmitter Antenna Gain
G_{r}	Receiver Antenna Gain
c	Speed of light
n	Pathloss Exponent
d_{o}	Close-in-reference distance
L_{t}	Transmitter feeder loss
L_{r}	Receiver feeder loss
d	Distance from transmitter to receiver
P_{r}	Received Power
d_{min}	Minimum distance
d_{max}	Maximum distance
h_{b}	Base station antenna height
h_{m}	Mobile antenna height
f	Frequency
$a(h_{\mathrm{b}})$	Correction factor
c_{m}	Correction factor
σ	Standard deviation
X_{σ}	Random number with zero mean and standard deviation
X_{f}	Correction factor for frequency above 1.5GHz
X_{h}	Correction factor for height of receiver antenna
s	Correction for shadowing
a, b, c	SUI Model Parameters

A_{fs}	Free space attenuation
A_{bm}	Median pathloss
K_0, K_1, K_2, K_3	Constants of Ericson Pathloss model
P_{jk}	Random Variable
P_{sens}	Power Sensitivity level
P_{o}	Received power at a reference distance

Chapter 1

Introduction

1.1 Overview

The commercial accomplishment of the wireless communication (WCS) system, since its introductory execution in the initial 1980s, has prompted an excessive interest among the engineers of telecommunication in understanding and estimating the characteristics of signal propagation in different environments. The impact of wireless technology has been and will continue to be profound. The future wireless communication system will provide the foundation for the modern society where equipment and people can be connected anytime and anywhere.

Wireless access network has come out to be a vital tool in managing the communications, particularly at home and working areas because of communication models. During the initial period of planning the communication system, propagation pathloss models (PLMs) are broadly utilized for conducting the feasibility studies. There are various prediction PLMs accessible to estimate the pathloss. The prediction PLMs have the main role in the optimization of signal coverage, analysis of interference and utilization of network resources efficiently [1].

Precise estimation of pathloss is important in the planning and designing of WCS. Such requirements are of great interest for mobile communication system designers to optimize the parameters of the system, for example, the location of base

stations (BTSs), level of interference and coverage of power, etc. Accurate prediction techniques are required to find these parameters of a mobile communication system that will improve the quality of service, lessen unwanted losses of power, increase the coverage region, and determine the arrangements of best BTSs of a specified region. The performance of WCS relies on the properties of the propagation channel.

Long-term evolution (LTE) deployment was initiated at the end of 2009, with goals to improve the standard of Universal Mobile Telecommunication System (UMTS) in order to cope up with the future needs [2, 3]. LTE can work in modern and more complicated arrangements of the spectrum. The evolution of high-speed packet access (HSPA) can operate on the bases of installed apparatus within the bandwidth of 5MHz. The fundamental requirement of a 3G and 4G LTE network is to fulfill the need for maximum coverage and quality targets. The maximum coverage means that the probability of availability of network service within the geographical location should be high. The important performance factors such as handover, received signal strength (RSS), rate of call success, the ratio of drop calls play a vital role in wireless mobile communication and these factors are related to quality targets. On the other hand, environmental factors like roads, geographical structure of the area, locations of different cites, should be taken into consideration during network planning [4].

1.2 Radio Propagation Path

Wireless communication channels are commonly defined by the four main characteristics of the propagation path namely, pathoss, shadowing, multipath delay spread, and multipath fading, as shown in Fig 1.1.

Between transmitter and mobile receiver, a signal attenuates during its transmission, this attenuation is known as the pathloss [5]. The signal power is decreased due to the different mechanisms such as refraction, reflection, scattering, diffraction, losses of free-space, etc. Multipath fading is one of the essential properties of the wireless communication medium. Fading is eventually the attenuation in the

RSS over different distances; also known as shadowing when the line of sight(LOS) is obstructed. A signal reaches its destination through various paths and distinct angles. The time difference between the first and last multipath received signal is known as delay spread [6].

The models that predict the signal and eventually the pathloss are known as the PLMs. The analysis of PLMs plays a vital role in theoretical and practical aspects. In this regard, the pathloss exponent (PLE) is one of the most important factors which have been considered in the analysis of the wireless communication channel. PLE is the monotonically decreasing rate of RSS with T-R distance and the value of PLE relies on propagation area. For the estimation of PLE, extensive measurements of RSS are used. Fluctuations in RSS occur due to shadowing is, in fact, the challenge in the estimation of PLE.

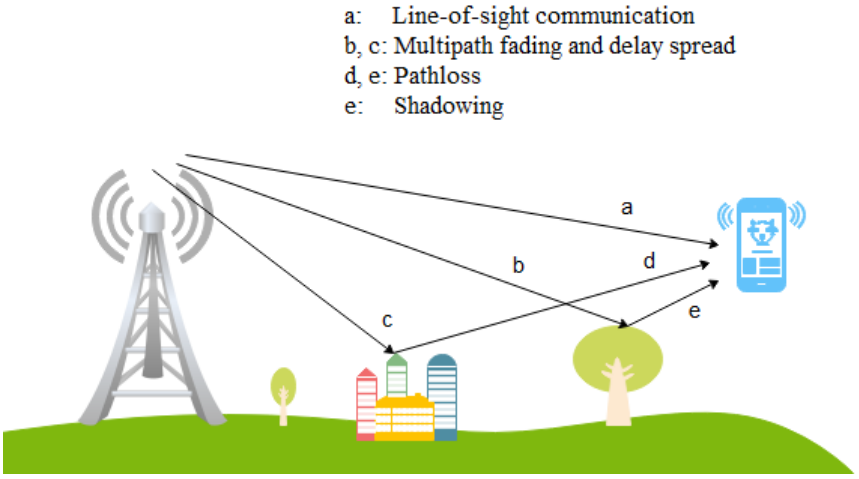

FIGURE 1.1: A typical wireless communication channel.

In a WCS, there is a need for enough understanding of wireless mobile communication systems, the ability to use suitable PLM among various propagation PLMs. To make sure the best performance of a cellular structure, the design of the network depends on the pathloss for designing and planning the wireless systems [7]. In the design and analysis of the WCS, the pathloss is investigated to be the most important factor [5]. The following block diagram represents the procedure of calculating the pathloss.

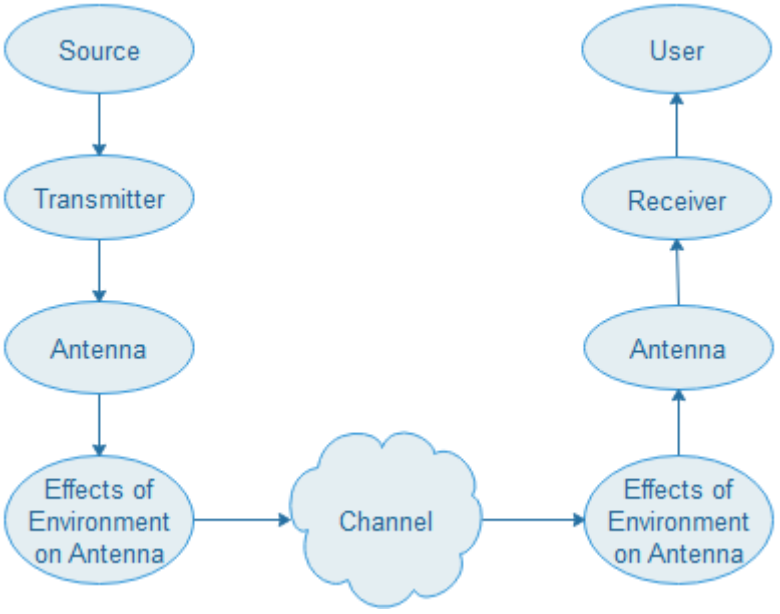

FIGURE 1.2: Block diagram for the calculation of propagation pathloss.

1.3 Radio Propagation Phenomena

1.3.1 Mechanisms of Signal Propagation

The electromagnetic signal is propagated through a channel by the following basic mechanisms [9],

- Reflection/Refraction
- Diffraction
- Scattering

1.3.1.1 Reflection/Refraction

When the propagation of electromagnetic wave starts, the reflection appears when a wave impinges upon a smooth surface (as shown in Fig 1.4(a)) or an object which has very large dimensions when compared to the wavelength of the propagating wave [10]. Reflection occurs due to many sources such as the surface of the ground,

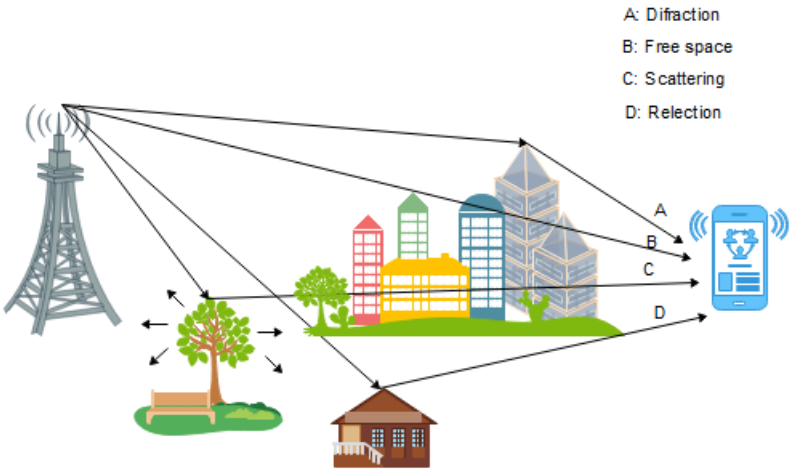

FIGURE 1.3: Propagation pathloss mechanisms.

buildings, the walls, equipment, and tall trees.

Because of the variations in air temperature, the density of the climate is changed. If the signal is affected by this kind of channel, the signal changes its direction from its original path and then refraction occurs (as shown in Fig 1.4(b)).

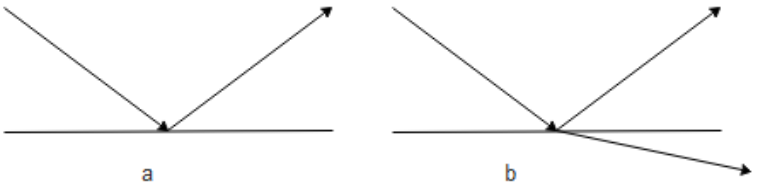

FIGURE 1.4: (a) Reflection (b) Refraction.

1.3.1.2 Diffraction

In wireless communication, diffraction occurs when propagation of wave starting from the BTS to the mobile terminal station(MTS) is obstructed with the sharp surface edge, as in Fig 1.5. When non line of sight (NLOS) present in the path of the signal, the signal propagates behind the obstacle through diffraction mechanism. Diffraction does not only depend on the geometry of obstacle but it also relies on the angle of the incidence, signal phase, and amplitude.

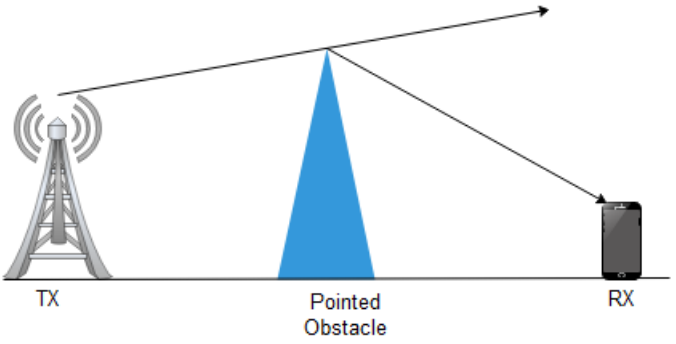

FIGURE 1.5: Diffraction mechanism.

1.3.1.3 Scattering

Scattering occurs when the channel consists of objects with dimensions that are small as compared to the wavelength and compared to the obstacles per unit is large enough as shown in Fig 1.6. In practice, scattering occurs because of small objects such as lamp posts and street signs in the city, etc.

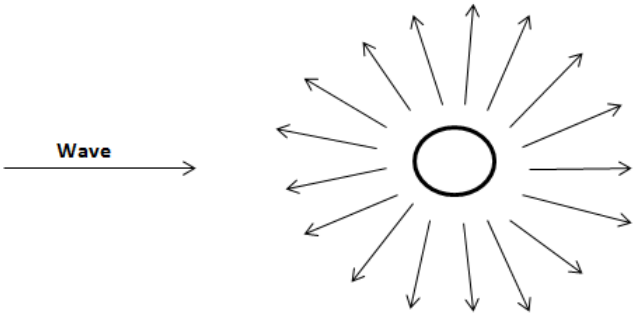

FIGURE 1.6: Scattering mechanism.

1.3.2 Received Signal Strength

The received signal strength (RSS) is a measure of how strong the received signal was when it reached its final destination. If the value of RSS is high, then a strong signal is received. If RSS value is very low then the WCS may fail. RSS is determined as [11]:

$$RSS = P_{\mathrm{t}} + G_{\mathrm{t}} + G_{\mathrm{r}} – PL – A \tag{1.1}$$

where, P_t is the transmitter power, G_t denotes the transmitter antenna gain, G_r represents the receiver antenna gain, PL is the pathloss, and A represents the cable and connector loss.

1.3.3 Pathloss

In wireless communication channels, the signal is suffered from attenuation while traveling from transmitter to receiver as shown in Fig 1.7. This attenuation is called pathloss. Pathloss is represented by a positive quantity measured in dB. The pathloss depends on the contours of the terrain, channel (dry air or moist air), area (urban, suburban, rural, and vegetation), the distance from a transmitter to receiver, and the antenna heights, etc [12]. The pathloss can be expressed as [13]:

$$PL(d) = PL(d_0) + 10n \log_{10}(\frac{d}{d_0}) \tag{1.2}$$

where, d represents the distance from BTS to MTS , d_0 denotes the reference distance from transmitter, and n is used to represent the PLE.

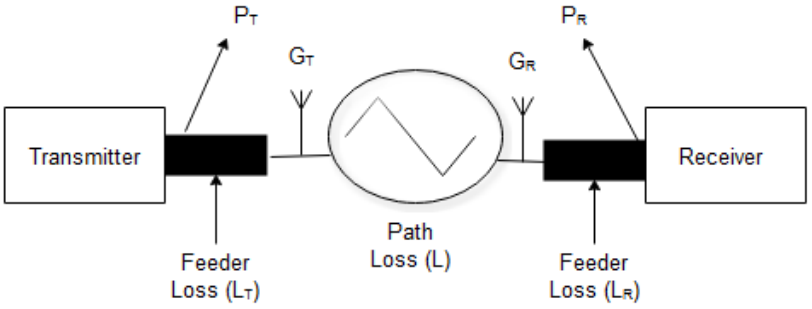

FIGURE 1.7: Pathloss phenomenon.

1.3.4 Pathloss Exponent/Pathloss Slope

In modeling of pathloss, PLE is one of the most important factors which have been considered in the analysis of the wireless communication channel. PLE is the

monotonically decreasing rate of RSS with distance and the value of PLE relies on the propagation area as presented in Table 1.1. For the estimation of PLE, extensive measurements of RSS are used. PLE can be calculated as [51]:

$$n = \frac{Pr(d_{\min}) - Pr(d_{\max})}{10\log_{10}(\frac{d_{\max}}{d_{\min}})} \tag{1.3}$$

where, $Pr(d_{\min})$ is the received power or RSS at the minimum distance (reference distance), $Pr(d_{\max})$ represents the received power or RSS at the maximum distance.

TABLE 1.1: PLE values in different areas [14, 50].

Type of Areas	**PLE**
Free space	2
Urban area	2.7 to 3.5
Shadowed urban region	3 to 5
Inside a building	1.6 to 1.8
Obstructed in a building	4 to 6
Obstructed in a factory	2 to 3

1.4 Necessity of Pathloss Models

It is essential to estimate the propagation characteristics of the system through the channel so that different parameters of a signal can be estimated more precisely in the mobile communication system. In WCS, it is very important to estimate the pathloss with maximum accuracy. In this regard, the propagation PLMs are the solution of estimating the pathloss with a small standard deviation. Hence, it will help the engineers and planners of the network to optimize the coverage area and to utilize the right transmit power. Furthermore, the types of equipment used to obtain the field measurements are very costly. Thus, propagation PLMs have been designed to estimate the pathloss as a less costly, suitable way and better

alternative. An accurate prediction PLM helps to optimize the transmitter power, coverage area and reduce the interference issues of other BTSs [9].

1.5 Pathloss Models

In WCS, information exchange from the transmitter to the receiver is accomplished through electromagnetic waves. Interaction between area and electromagnetic waves decreases the signal strength, which causes pathloss. Different PLMs are used to estimate the pathloss [7, 17]. Propagation models are classified in the following three categories,

1. Empirical Model
2. Deterministic Model
3. Stochastic Model

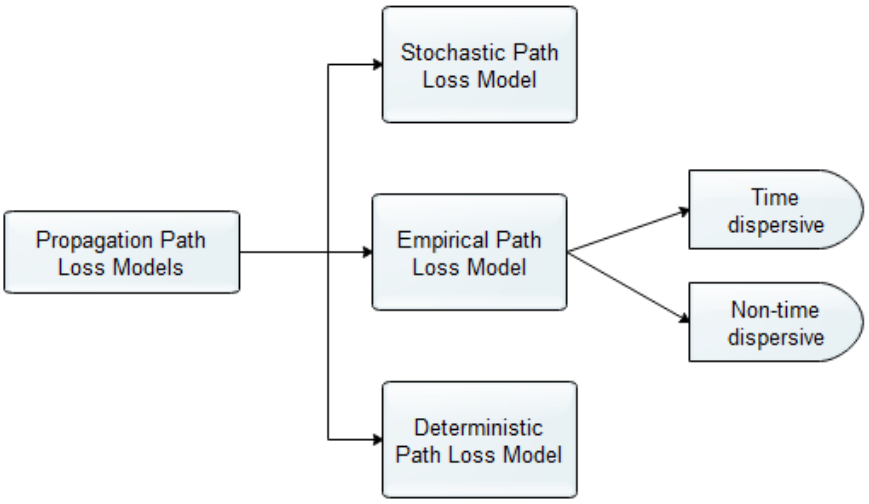

FIGURE 1.8: Different types of propagation PLMs.

Sometimes, it is difficult to define any random situation with the help of a mathematical model. Then, we use random data to observe the approximate behavior. An empirical model consists of algorithms and different mathematical equations

to perform the signal propagation. These models consist of a large number of measurements [15]. Empirical PLMs are further divided into two types such as time dispersive and non-time dispersive (as shown in figure 1.8). The time dispersive model gives us the information about the properties of time dispersive medium like channel having delay spread during the multipath effects [16].

The deterministic models utilize different laws to guide the electromagnetic signal propagation in order to find the RSS at an exact location. Mostly, deterministic models need a whole 3D map of the propagation area [15]. The modern system uses the specific site propagation model and graphical system model to predict the radio coverage of the signal. Designers of wireless system use the building databases to create the original presentation of the buildings and different features of the terrain. For the 3D representation of the building on the software, the ray-tracing technique is used [9].

Stochastic models are used to model different environments as a series of various random variables. Stochastic models need less information about the area but these models are the least accurate. Prediction of propagation pathloss for the frequency of 3.5GHz is done with the help of empirical and stochastic models [9, 15].

In this thesis, different PLMs are investigated in order to perform a comparative analysis of the measured pathloss with the theoretical PLMs. For this purpose, the following six PLMs are used and analyzed at a frequency of 1.8 GHz.

- Hata-Okumura Pathloss Model
- COST-231 Hata Pathloss Model
- Lognormal Shadowing Pathloss Model
- Stanford University Interim (SUI) Pathloss Model
- Ericson Pathloss Model
- ECC-33 Pathloss Model

1.5.1 Hata-Okumura Pathloss Model

The Hata-Okumura model [16, 19] is a very famous empirical PLM, which is based on the Okumura PLM and it is used to predict the RSS. The Hata-Okumura model is a well-developed model for the Ultra High Frequencies (UHF). The range of UHFs is between 300 MHz and 3 GHz. Previously, through the International Telecommunication Union recommendations (ITU-R), the ITU established this model for more extension up to 3.5 GHz. The Okumura model does not give any information for more than 3 GHz. By utilizing the information of the Okumura model, an extrapolated technique is applied to estimate the model for frequencies of more than 3 GHz. The Hata-Okumura model was developed by gathering a large amount of data in a city of Japan. Moreover, the Hata-Okumura PLM provides correction parameters for open and suburban environments [9]. The Hata PLM consists of equations based on the measurements and is derived from the curves of Okumura.

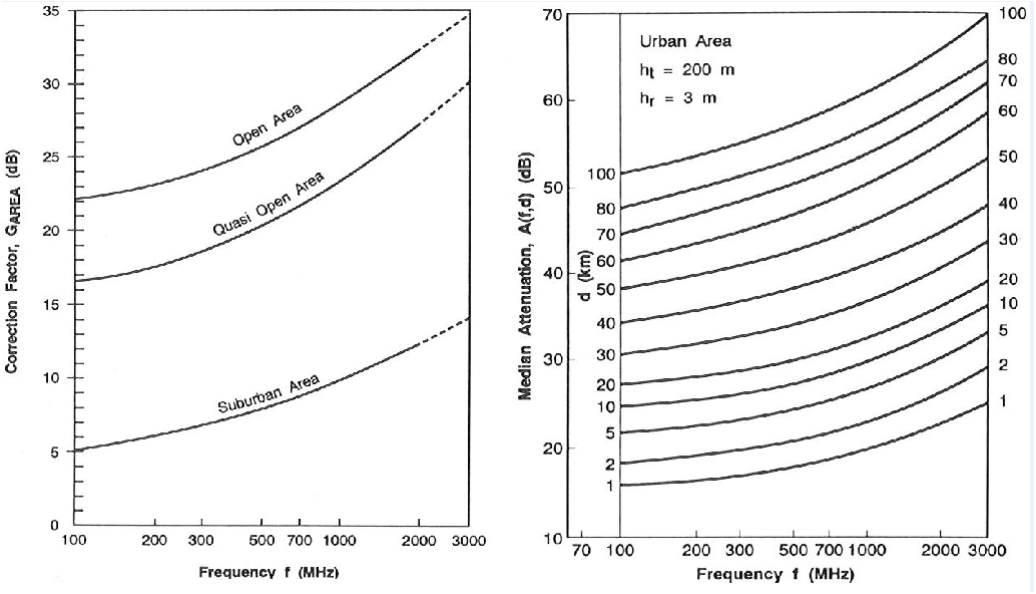

FIGURE 1.9: Attenuation factor for Okumura model [9].

Figure 1.9 shows that the base station antenna height gain G(hte) and the mobile antenna height gain factor G(hre) varies 20 dB/decade and 10 dB/decade, respectively. Hata proposed the standard formula of propagation pathloss for an urban

area, along with the correction factors to apply in other areas like suburban, rural, etc. However, the Hata-Okumura model does not consider the terrain profile between transmitter and receiver as both the Hata and Okumura assumed that transmitter would normally be situated on hills [21].

TABLE 1.2: Pathloss equations for different areas.

Area	**Pathloss Equation (dB)**
Urban	$A + B\log$ (d) - E
Suburban	$A + B\log$ (d) - C
Rural	$A + B\log$ (d) - D

where,

$$A = 69.55 + 26.16 \times \log(f) - 13.82 \times \log(h_{\mathrm{b}}) - a(h_{\mathrm{m}}), \tag{1.4}$$

$$B = 44.9 - 6.55 \times \log(h_{\mathrm{b}}), \tag{1.5}$$

$$C = 2 \times (\log_{10}(f/28))^2 + 5.4, \tag{1.6}$$

$$D = 4.78 \times (\log_{10}(f))^2 + 18.33 \times \log_{10}(f + 40.94), \tag{1.7}$$

$$E = 1.1 \times \log(f) - 0.7 \times (h_{\mathrm{m}}) - 1.56 \times \log(f) - 0.8, \tag{1.8}$$

where, f is the frequency in MHz, d represents the distance between BTS and MTS in meters, h_{b} is the height of BTS antenna in meters, h_{m} is the height of mobile receiver antenna in meters, and $a(h_{\mathrm{m}})$ is the correction parameter in dB. The effective height of MTS antenna $a(h_{\mathrm{m}})$ is defined in [21] as:

$$a(h_{\mathrm{m}}) = [1.1 \times \log(4)–0.7] \times h_{\mathrm{m}}–[1.56 \times \log(f)–0.8]. \tag{1.9}$$

Figure 1.10 shows the parameters of Hata-Okumura model.

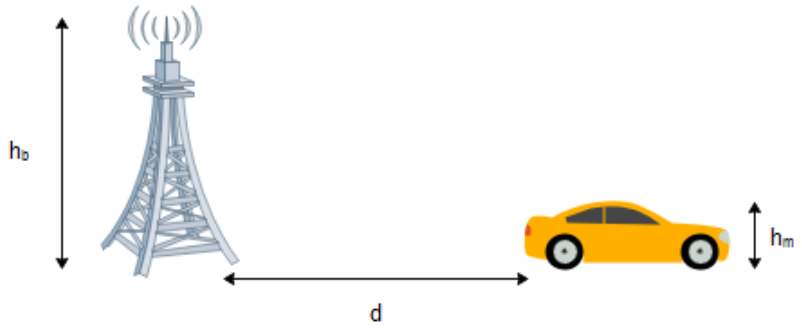

FIGURE 1.10: Parameters of Hata-Okumura model.

1.5.2 COST-231 Hata Pathloss Model

The Hata PLM is introduced as a mathematical expression to mitigate the best fit of the graphical information given by the old Okumura model [7]. Hata model is utilized for the frequency from 150 MHz to 1500 MHz to estimate the median pathloss for the distance from the transmitter to the antenna of the receiver up to 20 km. COST-231 Hata PLM is a combination of the F. Ikegami and J. Walfish model [24]. Moreover, COST-231 Hata model is preferable for the plane suburban and plane urban areas that have the same height of buildings [9, 23]. The COST-231 PLM is the expansion of the Hata-Okumura PLM. This model is used to estimate the pathloss in a wireless mobile communication system and it is suitable for frequency from 900 to 2000 MHz. COST-231 Hata model proposed the correction factors for suburban, rural, and urban areas. The basic equation of pathloss of this model is expressed as [24]:

$$PL(dB) = 46.3 + 33.9 \times \log_{10}(f) - 13.82 \times \log_{10}(h_{\mathrm{b}}) - a(h_{\mathrm{m}}) + (44.9 - 6.55 \times \log_{10}(h_{\mathrm{m}}) \times \log_{10}(d) + c_{\mathrm{m}} \tag{1.10}$$

where, f denotes the frequency in MHz, h_{b} is the height of BTS antenna in meters, h_{r} is the height of MTS antenna in meters, c_{m} represents the correction parameter and its value is defined according to area. As shown in Table 1.3, c_{m} and $a(h_{\mathrm{m}})$ are described for urban, suburban and open areas in [23, 25].

TABLE 1.3: Parameter and correction factors for different areas [25].

Area	**Correction Factor** c_{m}	**Parameter** $a(h_{\mathrm{m}})$
Urban	3dB	$3.2 \times (\log(11.75 \times h_{\mathrm{r}}))4.97$
Suburban	0dB	$(1.1 \times (0.7))h_{\mathrm{r}} - (1.56 \times (0.8)$
Rural	15dB	$(1.1 \times (0.7))h_{\mathrm{r}} - (1.56 \times (0.8)$

1.5.3 Lognormal Shadowing Pathloss Model

The measurement and theoretical based propagation PLMs are used to estimate the average RSS power reduced logarithmically with distance, whether it is in the outdoor or indoor radio medium. The amplitude of the signal changes due to the effects of shadowing and it is often modeled using the lognormal distribution. The meaning of Lognormal is that the local mean power is defined in the logarithmic scale. This model allows predicting the pathloss in a practical manner and also offers as the main advantage of the inclusion of all terms that influence the propagation. Fig 1.11 shows the effects of random shadowing over a large number of measurement locations which have a similar T-R separation, but different levels of clutter on the path of propagation is referred to as lognormal Distribution. This phenomenon is known as lognormal shadowing. In the log distance PLM, the average large scale pathloss for an arbitrary T-R separation is defined as a function of distance by using a PLE as shown in Equation (1.11). Variations in environmental clutter at different areas having a similar T-R separation aren't represented in the log distance PLM. This prompts that the estimated signals which are different from the mean values of RSS predicted by the Equation (1.11). In the lognormal shadowing model, Equation (1.12) is used to represent the variations in the measured data:

$$PL(d) = PL(d_0) + 10n \log_{10}(\frac{d}{d_0}), \tag{1.11}$$

$$PL(d) = PL(d_0) + 10n \log_{10}(\frac{d}{d_0}) + X_\sigma, \tag{1.12}$$

where, n represents the PLE. The value of PLE relies on the type of area. X_σ represents a random variable with zero mean and standard deviation of σ [26].

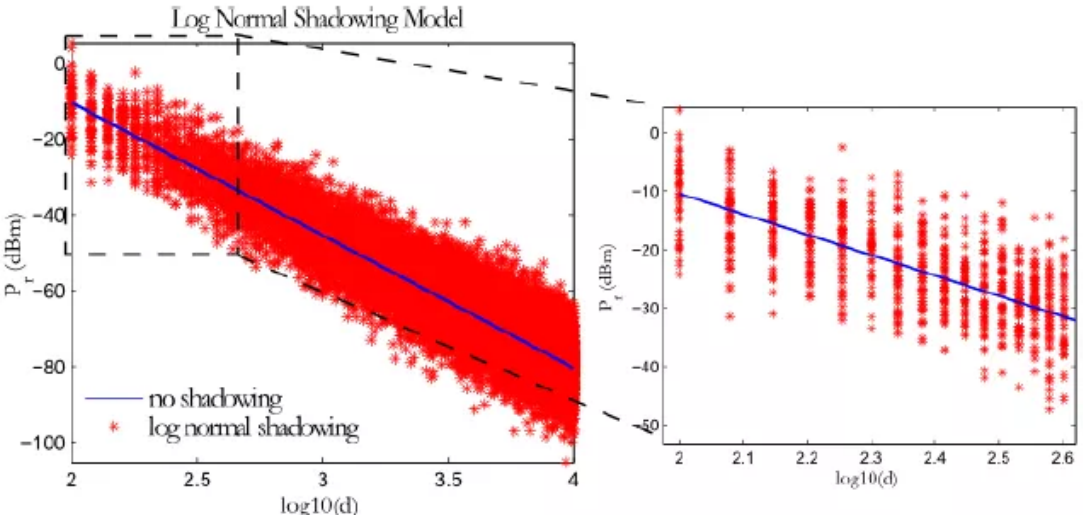

FIGURE 1.11: Result of lognormal shadowing PLM [26].

1.5.4 Stanford University Interim Pathloss Model

The development of the SUI model took place under the Institute of Electrical and Electronics Engineers (IEEE) 802.16 wireless access working group. This model originates from the expansion of the Hata PLM with a frequency band higher than 1.9 GHz. The correction factors are used to expand the SUI model up to the frequency of 3500 MHz. In SUI model, the ranges of antenna heights of transmitter and receiver are from 10 meters to 80 meters and 2 meters to 10 meters, respectively [21]. This model classifies three distinct kinds of terrain such as terrain A, B, and C. The terrain A is considered for the mountainous environment with heavy vegetation. In this terrain, the pathloss is the highest. Terrain B is used for the mountainous areas with very little vegetation and a flat area with dense trees while terrain C is used for plane areas or rural with very little vegetation. The basic pathloss equation with the correction parameters of the SUI model is presented as [16]:

$$PL = A + 10n\log_{10}(\frac{d}{d_0}) + X_{\mathrm{f}} + X_{\mathrm{h}} + s \qquad for \quad d > d_0 \tag{1.13}$$

where, d_0 denotes the reference distance in meters, X_{f} is the correction parameter for frequency over 1.5GHz, X_{h} is the correction parameter for height of receiver antenna in meters, s represents the shadowing correction parameter in dB, and γ denotes the PLE. The factors n, A, X_{f}, and X_{h} are presented as [16, 21]:

$$n = a - bh_{\mathrm{b}} + \frac{c}{h_{\mathrm{b}}}, \tag{1.14}$$

where the constant a, b, and c are given in Table 1.5.

$$A = 20\log_{10}(\frac{4\pi d_0}{\lambda}) \tag{1.15}$$

$$X_{\mathrm{f}} = 6.0\log_{10}(\frac{f}{2000}) \tag{1.16}$$

$$X_{\mathrm{h}} = \begin{cases} -10.8\log_{10}(\frac{h_{\mathrm{r}}}{2000}) & \text{for terrain A and B} \\ -20\log_{10}(\frac{h_{\mathrm{r}}}{2000}) & \text{for terrain C} \end{cases} \tag{1.17}$$

TABLE 1.4: Parameter values of different types of terrains.

Parameters of SUI Model	**Terrain A**	**Terrain B**	**Terrain C**
a	4.6	4.0	3.6
b	0.0075	0.0065	0.005
c	12.6	17.1	20

1.5.5 ECC-33 Pathloss Model

ECC-33 PLM was proposed by Electronics Communication Committee (ECC). Basically, it is extrapolated from the measurements of the Okumura model and the assumption of Okumura is modified in this model [27]. The initial test of the Okumura model was completed in the suburban locations of Tokyo. A typical European city is quite distinct from the characteristics of the environment of Tokyo which is a highly built-up city. The ECC-33 PLM is an empirical model which

consists of four terms and it can be defined as,

$$PL(dB) = A_{\text{bm}} + A_{\text{fs}} – G_{\text{t}} – G_{\text{r}}. \tag{1.18}$$

The factors A_{fs}, A_{bm}, G_{t}, and G_{r} are individually defined as [29]:

$$A_{\text{fs}} = 92.4 + 20\log(d) + 20\log(f), \tag{1.19}$$

$$A_{\text{bm}} = 20.41 + 9.83\log(d) + 7.89\log(f) + 9.56(\log(f))^2, \tag{1.20}$$

$$G_{\text{t}} = \log(\frac{h_{\text{b}}}{200})(13.958 + 5.8\log(d))^2. \tag{1.21}$$

For less urban area [28],

$$G_{\text{r}} = (42.57 + 13.7\log(f))(\log(h_{\text{r}}) - 0.585). \tag{1.22}$$

For large urban area,

$$G_{\text{r}} = 0.759h_{\text{r}} - 1.862. \tag{1.23}$$

1.5.6 Ericson Pathloss Model

In order to estimate the pathloss, the engineers of network planning used a software given by Ericsson organization to produce the Ericsson model. The Ericson PLM is formed on the improved version of Hata-Okumura PLM for different types of propagation areas according to parameters as shown in Table 1.6. According to this model, pathloss can be calculated as [30]:

$$\begin{aligned} PL = {} & k_0 + k_1 + \log_{10}(d) + k_2\log_{10}(h_{\text{b}}) + k_3\log_{10}(h_{\text{b}}).\log_{10}(d) - 3.2[\log_{10} \\ & (11.75h_{\text{r}})^2] + 44.49\log_{10}(f) - 478[\log_{10}(f)]^2 \end{aligned} \tag{1.24}$$

where, the values of k_0, k_1, k_2 and k_3 for distinct terrains are shown in Table 1.6.

TABLE 1.5: Ericsson PLM constants [30].

Environment	k_0	k_1	k_2	k_3
Urban	36.2	30.2	12.0	0.1
Suburban	43.2	68.93	12.0	0.1
Rural	45.95	100.6	12.0	0.1

1.6 Research Motivation and Objectives

The motivation of this work came from various research papers in which many researchers performed the comparisons of different propagation PLMs with field measured data. In various countries, researchers took data from different areas considering some selected aspects of the communication link and made its comparison with propagation PLMs. The PLMs have been a topic of interest for the researchers over the last three/four decades. As it will be discussed in the literature survey, a comparative analysis has been done in many countries such as Banta (Algeria), the state of Haryana (India), Kuala Lumpur (Malaysia), Japan, etc. To the best of our knowledge, no such analysis has been made for any area of Pakistan, which analyzes the communication link loss considering the behaviour of PLE.

This research is aimed to make a comparative analysis of the field measurements with different propagation PLMs like Hata-Okumura, ECC-33, COST-231, Log-normal shadowing, Ericson, and SUI models. In this thesis, six PLMs have been analyzed and used at a frequency of 1.8 GHz to estimate pathloss at different segments of a busy highway.

1.7 Thesis Organization

Organization of the thesis is in the following order;

Chapter 1: Introduction

This chapter gives an introduction about the propagation PLMs. In addition, the basic principles of propagation mechanisms are also discussed in this chapter.

Chapter 2: Literature Survey and Problem Formulation

This chapter presents a literature survey on the topics of comparison of propagation PLMs with field measurement data for distinct areas, multi-slope modelling and lognormal shadowing PLM. The literature survey is accompanied by a critical gap analysis of the research. This gap analysis then proceeds towards problem formulation. At the end of the chapter, research methodology and thesis contributions are presented.

Chapter 3: Field Measurements

This chapter presents the measurement setup, the softwares and hardware used, and the propagation area in which field measurements are obtained. The information and parameters of each BTS are also presented. Moreover, measured RSS and pathlosses are presented through simulations.

Chapter 4: Comparative Analysis of Field Measurements

This chapter presents the results found by the comparative analysis of PLMs with field measurements on the basis of pathloss. Moreover, the comparative study of PLMs in different countries is also analyzed. By the end of this chapter, a single slope PLM is presented.

Chapter 5: Multi-slope Lognormal Shadowing PLM

In this chapter, the multi-slope model is presented in two different ways, i.e., segmental multi-slope model and single-reference multi-slope model. Both multi-slope PLMs are also analyzed based on PLEs. Afterwards, the simulation results are presented to demonstrate the performance of the proposed segmental multi-slope lognormal shadowing PLM. At the end of this chapter, the distribution of field measurements is also discussed.

Chapter 6: Conclusion and Future Work

This chapter concludes the whole discussion made throughout this thesis and elaborates the future work.

Chapter 2

Literature Review and Problem Formulation

This chapter presents a literature survey on the topics of comparison of propagation PLMs with field measurement data for distinct areas, multi-slope modelling and lognormal shadowing PLM. The literature survey is accompanied by a critical gap analysis of the research. This gap analysis then proceeds towards problem formulation. At the end of the chapter, research methodology and thesis contributions are presented.

2.1 Background

Propagation PLMs have conventionally concentrated on estimating the RSS at a distance from the BTS. The prediction PLMs have a significant role in the optimization of radio frequency coverage, analysis of interference, and efficient usage of the available system resources [1]. Due to the pathloss, the power of the transmitted signal decreases, therefore, the analysis of the pathloss plays a vital role in both theoretical and practical aspects of wireless communication [32]. In WCS, there is a need for enough understanding to use suitable PLMs among various PLMs. In the cellular communication systems, accurate propagation PLMs help

us to identify the locations where new cell sites are required for providing the network coverage and provide acceptable cost estimation. On the other side, the estimation of inaccurate pathloss would either reduce the performance of the system or increase the cost of system [39, 40]. The performance of WCS relies upon the characteristics of the channel. The characteristics of the channel affect the design of the transmission strategy. PLMs and RSS play a vital role in the optimization of RF coverage. There are no universally accepted PLMs because the terrain conditions vary from place to place. It is needed to estimate the channel characteristics accurately in order to reduce the effects of interference. Therefore, extensive investigation on the effects of signal propagation pathloss has drawn a considerable attention [31].

The fundamental requirement of a 3G and 4G LTE network is to fulfill the need for maximum coverage and quality targets [33–35]. The maximum coverage means that the probability of availability of network service within the geographical location should be high. The important performance factors such as handover, RSS, rate of call success, and the ratio of dropped calls play a pivotal role in achieving the quality targets of any mobile communication system. On the other hand, environmental factors like roads, geographical structure of the area, location of different cites, should also be taken into consideration during network planning [4].

2.2 Comparative Studies of Propagation Models

A great amount of work has been done on the comparison of field measured data with theoretical PLMs in different countries. Several studies conducted in Banta, Malaysia, India, and other countries observed that various common PLMs performed less accurately when compared to field measurements. The results of the comparison of previous studies are discussed in this section.

2.2.1 Banta Algeria Study

In [6], the Banta city situated in Algeria was selected to obtain the field measurements for the comparative analysis of various PLMs. The comparison between measured pathloss and the predicted PLMs was done for two different BTSs (BTS1 and BTS2). For BTS1, the experimental data was taken in a radius of 1 km covering a rural area alongside, BTS2 covering the small area in a radius of 2.5 km and it is assumed that for adjacent BTSs handover occurs automatically, whenever the RSS is low. Special Huawei U6100 mobile phone, a laptop in which Huawei GENEX Probe software was installed, Global Positioning System (GPS) receiver (NMEA), and a receiving antenna were used for the collection of data. The experimental data was taken during driving a vehicle within the coverage area of BTSs while continuously recording the RSS. The parameters of the BTSs were taken from the "Mobilis" of Algeria for the analysis as shown in Table2.1.

TABLE 2.1: Parameters of the BTS used in Banta Algeria study [6].

Parameters	**Units**	**BTS1**	**BTS2**
Transmitted power	dBm	46	43
Gain of transmitter antenna	dBi	17.5	16.7
Gain of receiver antenna	dBi	0	0
Height of transmitter antenna	m	25	35
Height of MTS antenna	m	1.5	1.5
Frequencies	MHz	953	957.4

2.2.1.1 Equipment/Method used in this Measurements

The distribution system loss minimum reconfiguration technique using a genetic algorithm (GA) was proposed in [6] to optimize the empirical models properly and make it acceptable to the desired coverage area. In this technique, the number of iterations is reduced for distribution system reconfiguration. GA was used to

make an optimized closed solution with the help of acquiring the robust nature of genetics. By using the GA, new values were presented for the COST-231 PLM on the basis of field measured data.

2.2.1.2 Result of Comparative Analysis

The results of the Banta study show that for both BTS1 and BTS2, only the COST-231 PLM was found closer to the measured data. Hence, COST-231 PLM with proposed modification was recommended for Banta city.

2.2.2 Pondicherry-Villupuram Highway Study

The study in [38] proposed a propagation PLM for highway area between Pondicherry-Villupuram which is situated in Poondiyankuppam, Tamil Nadu. Comparative analysis of PLMs with field measurements obtained from Bharat Sanchar Nigam Limited (BSNL) for Pondicherry, India has been implemented. PLMs such as Hata-Okumura, COST-231 and ECC 33 models were analyzed and compared. The RSS was calculated regarding distance and model that can be adopted to reduce the number of handoffs and avoid effects of ping-pong were determined. The parameters shown in Table 2.2 were used in simulations of different PLMs.

TABLE 2.2: Values of parameters used in Villupuram highway study [38].

Parameters	**Units**	**Values**
Transmitted power	dBm	43
Height of Transmitter antenna	m	30
Gain of transmitter antenna	dBi	18
Distance from the transmitter to receiver	km	2
Height of Receiver antenna	m	3
Operating frequencies	MHz	1800

2.2.2.1 Equipment/Method used in this Measurements

E6474A Agilent model was used to find the number of RSS by using the mobile in the Pondicherry Villupuram highway. Agilent technologies give drive test solution and the E6474A model has the alternative of server-based software licensing. This model is used to keep up a pool of E6474A measurement licenses on a server and to contribute them to drive-test customer [39, 40]. Handover margins which have high RSS value can cause poor reception and this increase in the number of dropped calls. Meanwhile, handover margins that have low RSS value can give the "ping-pong effects". The ping-pong means handover to and fro between a cell pair frequently. The increasing rate of handover between cells within the same network leading to frequent dropped calls, network congestions and poor handovers in and around highways, require further investigation. Hence, the decision of handover was taken optimally from test drive adjacent cell RSS to decrease the ratio of dropped calls and the effects of ping-pong.

2.2.2.2 Result of Comparative Analysis

The results presented in the Pondicherry-Villupuram highway study show that the measured pathloss was best estimated by the Hata-Okumura PLM. Moreover, it was observed that the height of the transmitter is not directly proportional to the pathloss.

2.2.3 Kuala Lumpur(Capital of Malaysia) Study

Many studies conducted in different areas of Malaysia have observed that the commonly used PLMs perform less efficient when these propagation models are compared with measured values [42, 43]. In [44], four different sites were chosen in the Kuala Lumpur, Capital of Malaysia to obtain the measured data. The International Islamic University of Malaysia and the University of Putra Malaysia were chosen to acquire the measurements. In each university, two cell sites were

taken and all the measurements were taken during the daytime. The performance of PLMs like the ECC-33 model, Hata-Okumura PLM, the COST-231 PLM, SUI model, Egli model, Lee model, Lognormal shadowing model was compared with the measured data.

2.2.3.1 Equipment/Method used in this Measurements

Test equipment for the mobile system (TEMS) was used in obtaining the field measurements. TEMS is a technology used by operators of telecommunication to measure, analyze and optimize their mobile networks. Additionally, the system used the GPS and mobile handset of T610 in which TEMS software was installed. Ericson handset was used to find the RSS. There are three coordinates of the GPS receiver: Longitude, Latitude, and Altitude. These coordinates were synchronized with the level readings of received power.

2.2.3.2 Result of Comparative Analysis

From the outcomes of the Kuala Lumpur study, it can be observed that the lognormal PLM gave good results for the smaller distances. Moreover, ECC-33 and Lee PLMs were overestimating the values of measured pathloss whereas, COST-231 and Egli were underestimating the measured pathloss values.

2.2.4 South-South Part of Nigeria Study

This research presented in [45] attempts to find the most suitable propagation PLM in the South-South part of Nigeria. Two different cell sites operating at the frequency of 900MHz and 1800MHz were used for the experiment in an urban area. For comparison of field measurements with existing PLMs, the pathloss was measured and then the measured pathloss was compared with the theoretical PLMs like the Hata-Okumura, Cost-231, SUI, Ericsson, and Free Space. The parameters shown in Table 2.3 were used in simulations of different PLMs.

TABLE 2.3: Simulation parameters used in Nigeria study [45].

Parameters	**Units**	**Values of cell site-1**	**Values of cell site-1**
Transmitted power	dBm	40	40
Gain of transmitter antenna	dBi	17.5	17.5
Height of transmitter antenna	m	40	42
Height of mobile antenna	m	1.5	1.2
Frequencies	MHz	900	1800

2.2.4.1 Equipment/Method used in this Measurements

Ericsson k800i testing equipment was used for site verification, and calls were made at each test point until it established and the information of RSS sent over the air interface between the transmitter and the receiver was read. For each site, RSS was measured at a reference distance of 200m from the transmitter and a subsequent interval of 200 meters up to 2000 meters.

2.2.4.2 Outcomes of the Comparative Analysis

The outcomes presented in the South-South part of Nigeria study show that the variations exist between field measurements and the existing empirical PLMs. However, a slight difference in COST-231 model was observed at the distance of 1.4km and 1.2km in both site-1 (900MHz) and site-2 (1800MHz) respectively. Results proved that the COST-231 model was found very effective for the radio wave propagation pathloss prediction in the South-South part of Nigeria.

2.2.5 Advanced Three Dimensional Computations of Pathloss Models

The vehicle to vehicle (V2V) and vehicle to infrastructure (V2I) communication has increased with the requirement of Vehicular Ad-hoc Networks (VANETs) and

small traffic Systems. In [46], simulations of the propagation PLMs in V2V and V2I networks used in the smart Traffic System was presented. For MATLAB based simulations of PLMs, advanced three dimensional (3D) computations of PLMs, environment scenario and power delay profile (PDP) were used. The simulation of PLMs in V2V and V2I wireless communication showed accurate results as compared to actual experimental outcomes presented in [47]. A complicated simulation scenario was represented very easily by using such simulations whereas real experimental setup is not feasible.

2.2.6 Tuning of COST-231 Model

The tuning of PLMs is a significant problem in the planning of an efficient network. The study in [48] proposed a tuning method of the COST-231 PLM to maximize the accuracy of the PLM. This method is based on obtaining a large number of RSS measurements using the LTE technique. The measurements of RSS were used in their study presented in Table 2.4. The predictions pathloss of the tuned model was then compared with the COST-231 PLM. On the basis of LTE measurements obtained from mobile devices, they developed a hardware and software system to find the correction factors for the propagation PLM. The calculation of the correction factor of the COST-231 PLM was found to be 13.3 dBm.

TABLE 2.4: Comparison between the theoretical and experimental values of RSS [48].

Coordinates (Lat,Long)	**Theoretical values (dBm)**	**Experimental values (dBm)**
55.0128,82.9508	-73	-90
55.0122, 82.95	-91	-105
55.0125,82.9492	-96	-97
55.0128,82.9481	-104	-113
55.0133,82.9470	-108	-92
55.0129,82.9493	-90	-118

2.2.7 Haryana (State of India) Study

In [49], three different locations were selected in Haryana (state of India) to obtain field measurements. Their test measurements were carried out in an urban, sub-urban and rural areas at 900MHz and 1800MHz frequency. Authors carried out a drive test by using spectrum analyzer tool and they successfully measured the pathloss values for various terrains. They considered the SUI model, Log distance PLM, Hata-Okumura PLM, ECC-33 model, and COST-231.

2.2.7.1 Result of Comparative Analysis

As presented in their results, the SUI model and ECC-33 model showed the perfect output in an urban area. COST-231 pathloss, ECC-33, and SUI PLMs showed the acceptable result in a suburban environment. The HATA-Okumura PLM gave good results in the urban and suburban environments whereas the HATA-Okumura and Log distance PLMs gave better results in the rural environment.

2.3 Related Studies about Multi-slope Modelling and Lognormal Shadowing Model

2.3.1 Resource Optimization Exploiting Multi-slope Pathloss Model

The research in [56] analyzed different multi-slope PLMs, where different communication links are characterized by various PLEs. The authors proposed a system for joint user association, subcarrier and power allocation on the downlink of a heterogeneous network (HetNet). They compared the performance of the proposed method under various PLMs with shown effectiveness of dual slope PLM in comparison to the single slope PLM. They deduced that the dual slope PLM

shows significant improvement in the performance of the network as compared to the single slope PLM by estimating the PLE accurately on the distance.

2.3.2 Downlink Network Analysis with Multi-slope Pathloss Model

In [57], the authors analyzed the probability of network coverage and potential throughput under the multi-slope PLM. They focused on the function of dual slope PLM, which is used to accurately estimate various practical scenarios. The distributions of SIR, SNR, and SINR before finding the potential throughput scaling was derived. The outcomes show that the SIR decreases with network density, while the converse is true for SNR, and thus the network coverage probability in terms of SINR is maximized at some finite density.

2.3.3 Modeling of Indoor Channel using Multi-slope Modeling

This research [53] presented a log distance multi-slope model and the indoor distribution of pathloss. In normal and lognormal distributions, the value of standard deviation defines various effects of fading. The particle swarm optimization (PSO) method was used to find the mean square error (MSE) and MSE was optimized using multi-slope models. In the multi-slope model, parameters of the channel were determined using the empirical values collected in [37, 54, 55]. Outcomes of distributed pathloss were processed with the help of the PSO algorithm to optimize the normal and lognormal distribution. The multi-slope model was estimated by using the PSO algorithm at frequency f = 2.5 GHz. For the normal distribution, the deviation error of 15.9 dB was achieved after optimization.

2.3.4 Modeling of Indoor Signal Propagation using Lognormal Shadowing

The study in [50] analyzed the distribution of field measured data. Alongside, the accuracy of the lognormal shadowing PLM by showing the relationship between the T-R distance and RSS was presented. The characteristics of slow fading were measured, with effects of shadowing as well as without effects of shadowing by considering the lognormal distribution. At the frequencies of 2.4 GHz MHz and 5 GHz, RSS was measured at different distances.

On the second floor of a building, three rooms and hallways and one hallway on the first floor were chosen as locations. The first data was recorded at a distance of 0.5m away from the access point. This access point was considered as the close-in-reference distance d0. RSS was recorded at 2 meters up to 24 meters in the case of LOS. NLOS measurements were obtained at different intervals. The values of n = 2.31 and $\sigma = 6.42$ were calculated by using the measurements gathered during the field survey. They deduced that the measured data were distributed normally because the 95% data fall in 2σ. So, they concluded that over distance up to 30m the model provides accurate results.

2.3.5 Pathloss Exponent Estimation using One Line Measurement and Gradient Descent Technique

The study in [51] presented two types of techniques for the estimation of PLE. These techniques were One line measurement and gradient descent technique. In one line measurement, PLE was found by using the extensive measurements of RSS and distances. The other technique is to renovate environmental factors directly with the help of the gradient descent method. In gradient descent technique, RSS is randomly measured as long as the locations are exactly known and this technique is also known as online update measurement as the PLE can be upgraded continuously. The values of RSS were gathered by locating the BTS and MTS along a straight line. In one line measurement technique, obtained RSS was

marked on a straight line. Received power at reference distance Pr (d_0) was taken at different locations by moving both transmitter and MTS at the same time for all the positions and directions. The mean value was measured to be -35 dBm. The difference of maximum and minimum RSS was measured (-35 + 62 = 27 dB). The value of PLE was $n = (27/9.5424) = 2.83$.

For the online update technique, the authors performed three different tasks:

- Task 1: Measurement of predesigned spread,
- Task 2: Measurement from small-to-big rectangular,
- Task 3: Measurement from big-to-small rectangular.

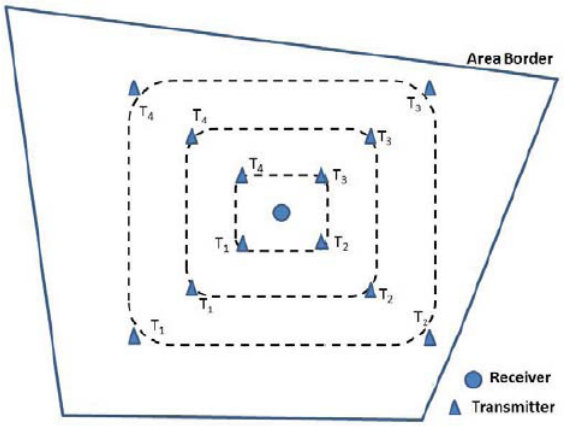

FIGURE 2.1: Rectangular shaping [51].

The area in which the measurements were taken can be in any type of shape. The allocation of four different transmitters always made a rectangular shape to include the mobile receiver at mid of the rectangle. For every location, ten training cycles were observed. For calibration, a total of 110 training cycles were used. For each cycle, the value of PLE was measured.

2.3.6 Pathloss Exponent Estimation using VariLoc Ranging Algorithm

Due to channel fading, measurements of RSS are known as unreliable parameters for the estimation of PLE and localization. To solve this problem, the research in [32] presented a ranging technique known as VariLoc. The variLoc method is depending on the beacon's transmitting power and Psens for ranging instead of considering RSS. The advantage of variLoc ranging is to consume the low power by reducing the transmission power to find RSS ' is approximately equal to Psens. The receiver can utilize averaging over many measurements of RSS sent at different times with different powers to decrease the variation in RSS [52]. They analyzed that depending on a very less transmission power can fulfill the connectivity need of the receiver and it was more robust against multipath fading and environmental change.

2.4 Research Gap and Problem Formulation

As discussed in the literature survey, there are several studies on the comparison of PLMs with field measurements in different countries, but we have not been able to identify any comprehensive study on 4G LTE pathloss modelling for any area of Pakistan. The efficiency and accuracy of existing models are limited when they are deployed for an environment that is different in terms of geographical formation from that for which they have been designed. Therefore, it is required to investigate pathloss models for their suitability for accurate signal estimation in particular areas of Pakistan.

Hence, this work is focused to investigate the performance of the most commonly used predictive PLMs by comparing them with field measurements for three different sites on the Islamabad Expressway, Pakistan. Based on the comparison, a best fit predictive PLM is further modified and it validates the accuracy of the modified model for improved pathloss estimation in a similar area.

Most literature on the performance analysis of cellular networks uses single slope

PLM to characterize the physical propagation environment. However, the massive data traffic in WCS leads to increasing network uncertainties, which cause variations in the links significantly. Hence, it is required to employ PLMs that account for the variation in the environment. ***This work is an attempt*** to fill this gap by considering a multi-slope PLM and validating it with our measurements to overcome the shortcoming of single slope PLM.

Although a great amount of work has been done on the lognormal shadowing model and multi-slope modelling separately, according to the best of our knowledge, there is not even single literature in which the lognormal shadowing PLM has been implemented on the multiple slopes for the outdoor environment.***In this thesis,*** the multi-slope lognormal shadowing PLM is proposed for the outdoor environment to improve the performance of single slope lognormal shadowing PLM. All previous efforts to take measurements were by using complex software and costly equipment such as a spectrum analyzer, laptop with Ericsson software, a network communication analyzer (ACTIX analyzer 4.05) software, and GPS receiver, etc. ***In this research work,*** a simple and inexpensive way to measure the field data is presented. A Net-Track Lite and Cell mapper applications are used during the site surveys.

2.5 Research Methodology

In the first phase of the research, field measurements are aimed to be collected. For this purpose, three sites are chosen on Islamabad Expressway, Pakistan. A drive test is conducted with the help of a cell phone Samsung A50 pre-installed with g.net track lite and cell mapper applications and enabled LTE sim. The vehicle is driven at a speed of 50 km per hour while the cell mapper recorded the RSS continuously. The 100 measurements are taken at 0.1 km, 0.2 km, 0.3 km up to 4km, 2km and 2km for site-1, site-2, and site-3 respectively. By utilizing the field measurements, the pathloss is analyzed for each site in MATLAB software. For comparison and analysis, existing PLMs such as Hata-Okumura, ECC33, COST-231, Ericson, SUI, and Lognormal shadowing models are analyzed in MATLAB. Finally, a comparison

of predictive PLMs with measurement results is made on the basis of pathloss. Based on the comparison, the best-estimated PLM is proposed. Afterwards, we perform a comparison of single slope PLM with multi-slope PLM. In this regard, the multi-slope lognormal shadowing PLM is proposed. Moreover, the distribution of field measurements is analyzed by using the lognormal distribution.

2.6 Thesis Contributions

Major contributions of this thesis are listed as under:

- To obtain the field measurements, a drive test is conducted for three different cell sites selected on Islamabad Expressway, Pakistan. By utilizing the field measurements, the pathloss is measured.
- Field measurements are compared with the theoretical PLMs such as the Hata-Okumura model, ECC-33 model, COST-231 Hata model, SUI model, Ericson model, and Lognormal shadowing model.
- The theoretical models that are considered in this thesis are primarily based on single slope PLM. Since the pathloss is not accurately estimated by single slope PLM, therefore, a multi-slope PLM is used to overcome the shortcoming of single slope PLM.
- Multi-slope PLM is used in two different ways, i.e., segmental multi-slope PLM and single-reference multi-slope PLM. The estimation of PLE is done by using both multi-slope PLMs. On the basis of estimated PLEs, a comparison is drawn between segmental and single-reference multi-slope PLMs.
- The lognormal shadowing PLM is evaluated under segmental multi-slope model and proves that the multi-slope model improves the performance of a cellular network in comparison to the single slope model. Moreover, we investigate the distribution of field measurements by using lognormal distribution.

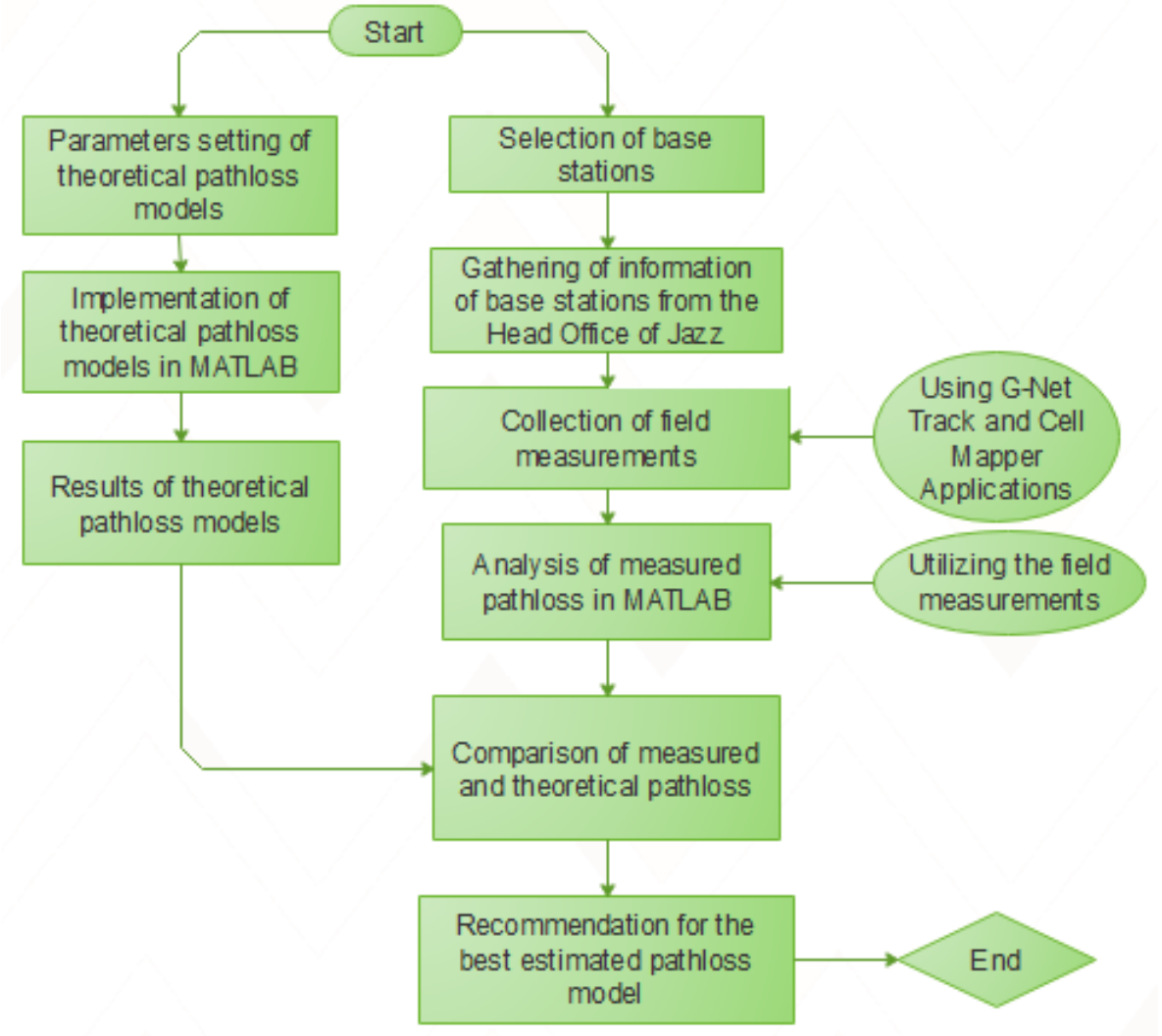

FIGURE 2.2: Flow chart of comparison of pathloss models with field measurements.

Chapter 3

Field Measurements

To check the efficiency of predictive PLMs, the comparative analysis between measured and calculated values was required and for comparison, the field measurements were needed. Hence to obtain the field measurements, the selection of BTSs is very important. In this chapter, a detailed description of the measurement setup, field measurements, information of BTSs and equipment used during the collection of field measurements are presented.

3.1 Measurement Setup

3.1.1 Site Geography

The Islamabad Expressway, Pakistan was selected to obtain the field measurements. This Expressway passes from north to south as shown in Fig 3.1 and provides quick access between Islamabad and Rawalpindi city. Three BTSs were chosen as the sources of signal to obtain the field measurements on the Islamabad Expressway. These BTSs were in Koral Town, Korang Town, and Soan Garden as shown in Fig 3.2, 3.3 and 3.4, respectively. The selected terrains have the availability of less vegetation and houses or buildings mostly below 20 meters.

FIGURE 3.1: Selected base stations on Islamabad Expressway.

3.1.2 Measurement Procedure

At three different locations on the Expressway, data was collected when driving a vehicle. The testing tool used to obtain the field measurements was Samsung mobile A50 in which pre-installed the G.Net track lite and cell mapper applications. RSS values were recorded at various distances from each of the three BTSs, named as BTS1, BTS2, and BTS3. Measurements were taken within the frequency of 1.8 GHz at intervals of 0.1 km, after an initial separation of 50m away from BTS1, BTS2, and BTS3. The area covered by BTS1, BTS2, and BTS3 was 4 km, 2 km, and 2 km, respectively. The exact locations of BTSs were found by using the latitudes, longitudes, and cell-id of each tower as shown in Table 3.1.

As shown in Table 3.1, the information of each tower, such as cell identity, latitude, and longitude, was obtained from the Head office of "Mobilink" Islamabad for analysis.

FIGURE 3.2: Image of BTS1 used (Koral town).

FIGURE 3.3: Image of BTS2 used (Korang town).

FIGURE 3.4: Image of BTS3 used (Soan garden).

TABLE 3.1: Information of selected base stations.

Base Station	**Location**	**Coordinates(Lat,Long)**	**Cell-Id**
BTS1	Koral Town	33.60932747, 73.13341261	RWP-26131
BTS2	Korang Town	33.57845253, 73.15050676	RWP-13303
BTS3	Soan Garden	33.56592995, 73.15608449	RWP-07001

3.1.3 Base Stations Parameters

Table 3.2 presents the parameters of the selected BTSs. These parameters were used in analyzing the field measurements in MATLAB. The parameters regarding each BTS including the transmission frequency, transmitted power, height of antenna, EIRP, and BTS antenna gain were obtained from the headquarter of "Mobilink" located in F8 Islamabad.

TABLE 3.2: Parameters of selected base stations.

Parameters	**Values**
BTS Transmitting power	47 Watts
MTS antenna height	1.5m
BTS antenna height	60m
BTS antenna gain	15dBi
MTS antenna gain	1dBi
Operating frequency	1.8 GHz
EIRP	62dBm

3.1.4 Equipment and Software Used

The hardware used to gather the measurements was samsung A50 mobile phone. The following applications were used to obtain the field measurements:

- G-Net Track Lite.
- Cell Mapper.
- Google Earth Map.

G-net track application is a wireless monitor and drive test tool for android mobile devices. This application allows monitoring and logging of mobile network parameters without using specialized tools [62]. Cell mapper is a cellular coverage application. In this application, we can check our own provider mobile network coverage. Also, we can see our provider mobile locations of the tower on the map [63]. The google earth map is a 3D representation of earth-based primarily on satellite imagery. This can be used to measure the exact distances between different sites.

3.2 Field Measurements for Comparative Analysis

3.2.1 Measured Received Signal Strength

The values of the RSS were taken at an interval of 0.1 km as shown in Appendix Table A.1 to A.3. The 100 measurements are taken at distances of 0.1 km, 0.2 km, 0.3 km up to 4km, 2km and 2km fixed length for BTS1, BTS2, and BTS3 respectively. For each BTS, RSS was started to record at a reference distance of 50 meters from the BTS. By using the field measurements, the average values of RSS for each interval are obtained and these average values were used in simulations. The results of measured RSS are graphically presented in Fig 3.5, 3.6, and 3.7 for three locations: Koral town, Korang Town and Soan garden, respectively. The results show decreasing trend of RSS with respect to distance. From the result depicted in Fig 3.10, it is analyzed that the RSS increases significantly from a distance of 0.1 km up to 0.4 km and then starts decreasing with T-R separation distance. There is might be no shadowing in that particular region which causes the RSS to increased.

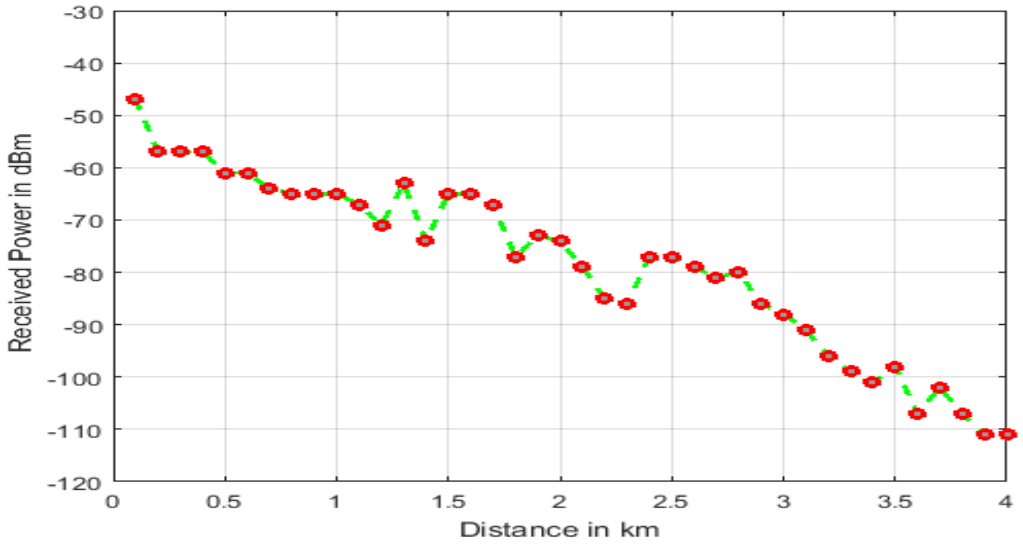

FIGURE 3.5: Measured RSS from BTS1 located in Koral town.

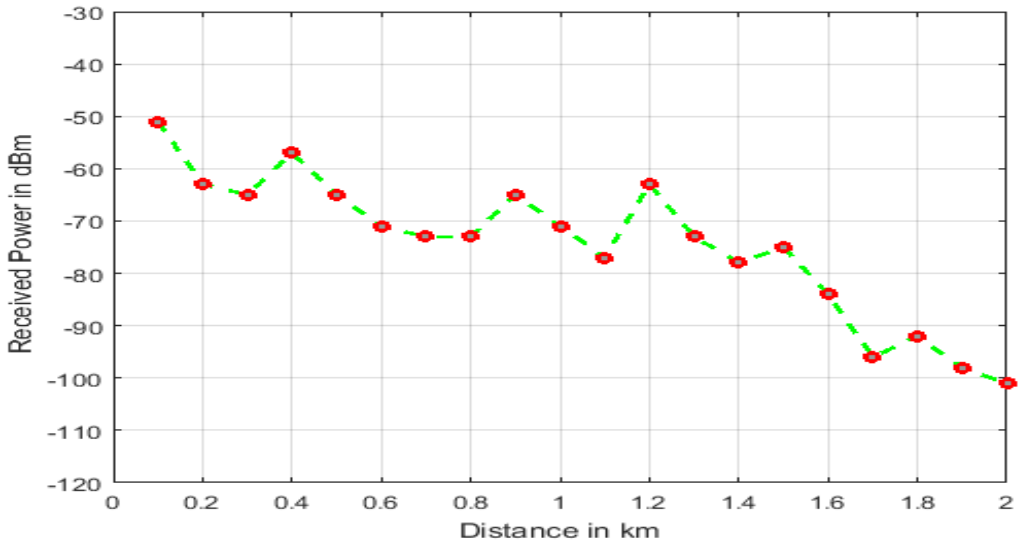

FIGURE 3.6: Measured RSS from BTS2 located in Korang town.

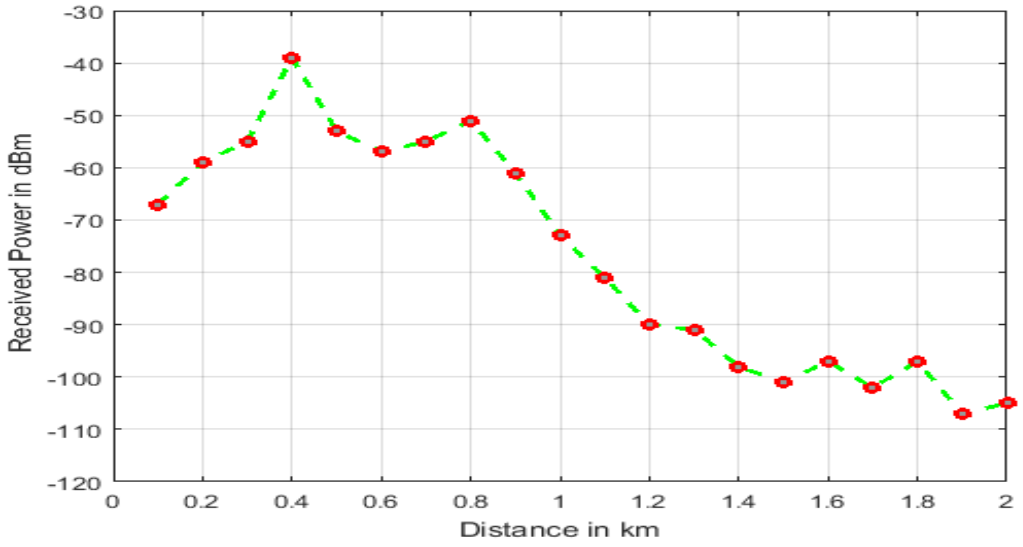

FIGURE 3.7: Measured RSS from BTS3 located in Soan garden.

3.2.2 Measured Pathloss

By utilizing the measurements of RSS, pathloss was analyzed and graphically presented against separation distance for each BTSs in MATLAB. For each value of measured RSS, the corresponding pathloss was calculated using the following equation:

$$L(measured) = EIRP - P_{\mathrm{r}} \tag{3.1}$$

where L represents the pathloss, P_r is the measured RSS and $EIRP$ is effective isotropically radiated power and it is used to represent the product of antenna gain and transmitted power.

$$EIRP = G_{\mathrm{t}} \times P_{\mathrm{t}} \tag{3.2}$$

where, G_{t} is the BTS antenna gain and P_{t} represents the transmitted power. Figures 3.8 to 3.10 illustrate the increasing trend of pathloss with distance. The result of driving test performed in the area of Koral town, Korang town, and Soan garden observed a mean pathloss of 139 dB, 136.55 dB, and 138.55 dB, respectively. From Fig 3.10, it is observed that the pathloss reduces significantly from distance of 0.1 km up to 0.4 km and then shows the increasing trend. There is might be no shadowing in that particular region which causes the pathloss to decreased. The maximum values of pathloss were found 173 dB, 163 dB, and 167 dB for Koral town, Korang town, and Soan garden, respectively.

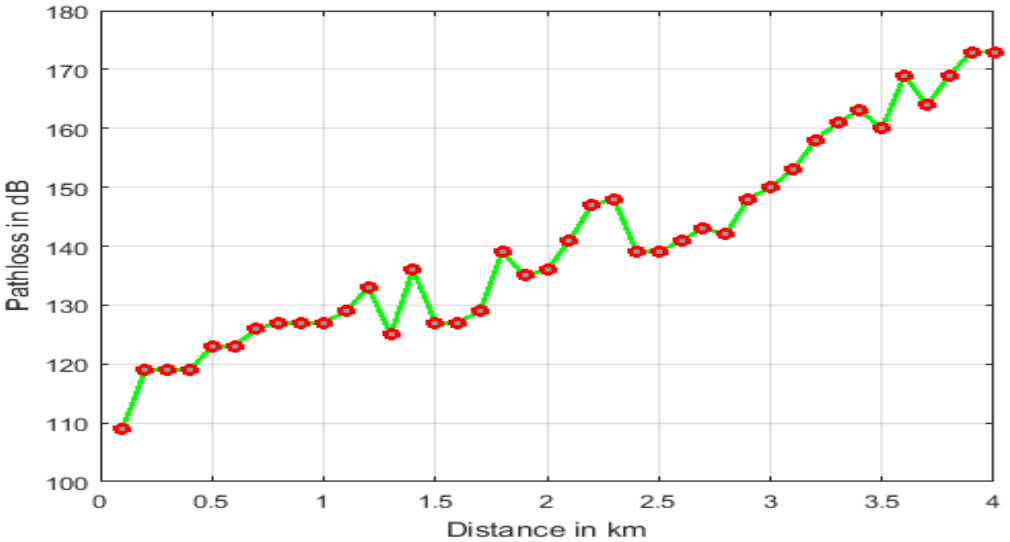

FIGURE 3.8: Measured pathloss from BTS1 located in Koral town.

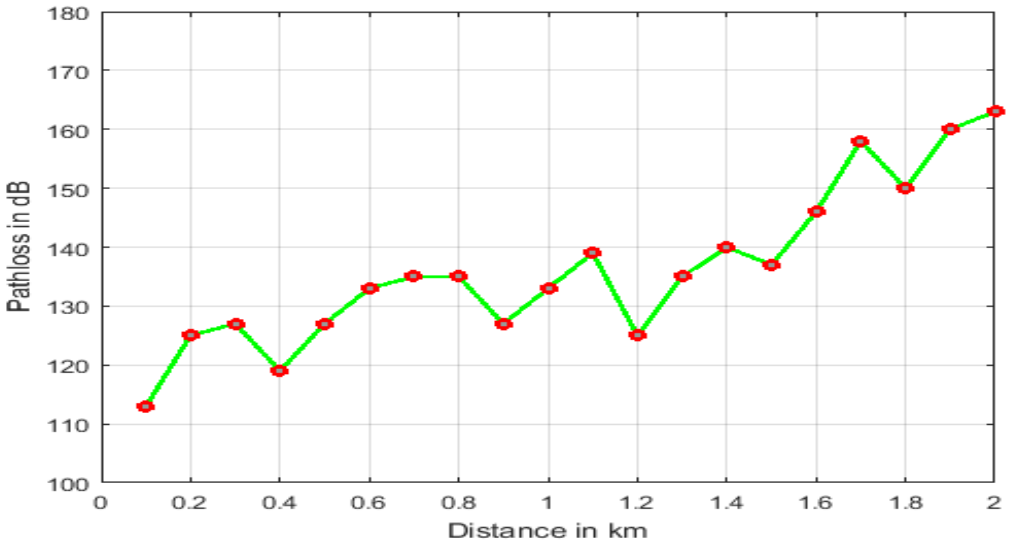

FIGURE 3.9: Measured pathloss from BTS2 located in Korang town.

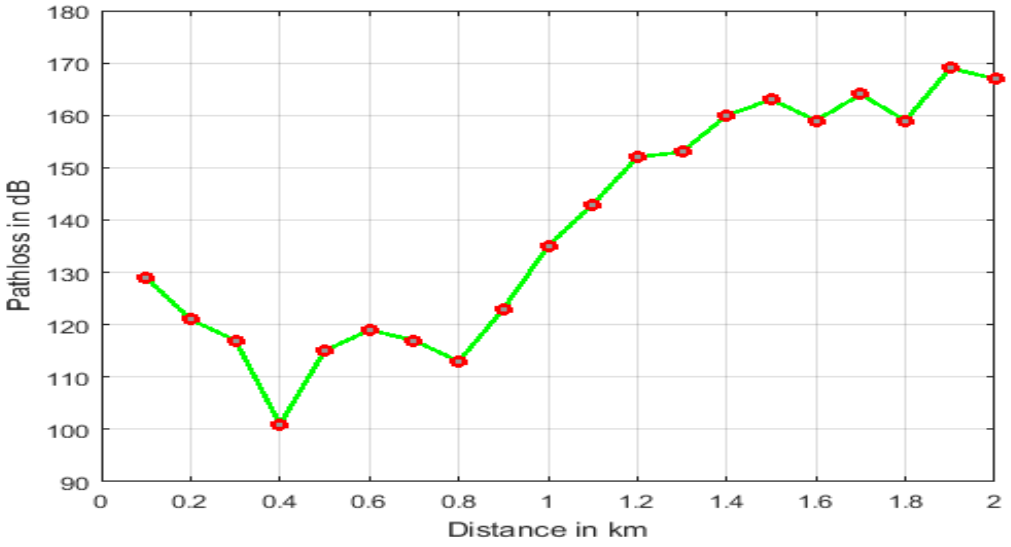

FIGURE 3.10: Measured pathloss from BTS3 located in Soan garden.

3.3 Measured RSS at various Distances for Estimation of Pathloss Exponents

In WCS, the massive data traffic and densification lead to growing network uncertainties, which significantly cause the variations in the communication links. These variations occur due to many physical factors such as ground reflections, link distances, scattering, and interference, make pathloss modeling a difficult task

in wireless networks. To analyze these variations in field measurements of RSS, over ten thousand measurements were obtained at different distances as shown in Fig 3.13 to 3.17.

The measurements were obtained at distances of 50 m, 500 m, 1000 m, 1500 m, 2000 m, 2500 m, 3000 m, 3500 m, and 4000m. Hence, for every distance, there are a thousand values of RSS. By utilizing the measurements of RSS, the average values of RSS are obtained. These average values of RSS are utilized to calculate the PLE and analyze how the PLE changes with variations in RSS (presented in Chapter 5). From Fig 3.11 to 3.15, it is observed that there are variations in the field measurements with respect to distance.

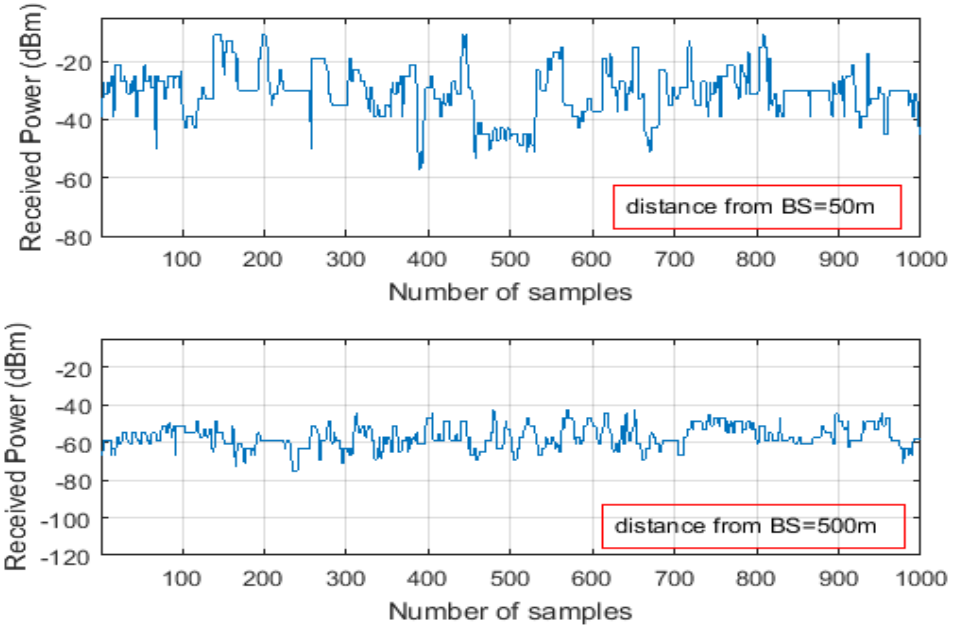

FIGURE 3.11: Measured data at 50 and 500 meters.

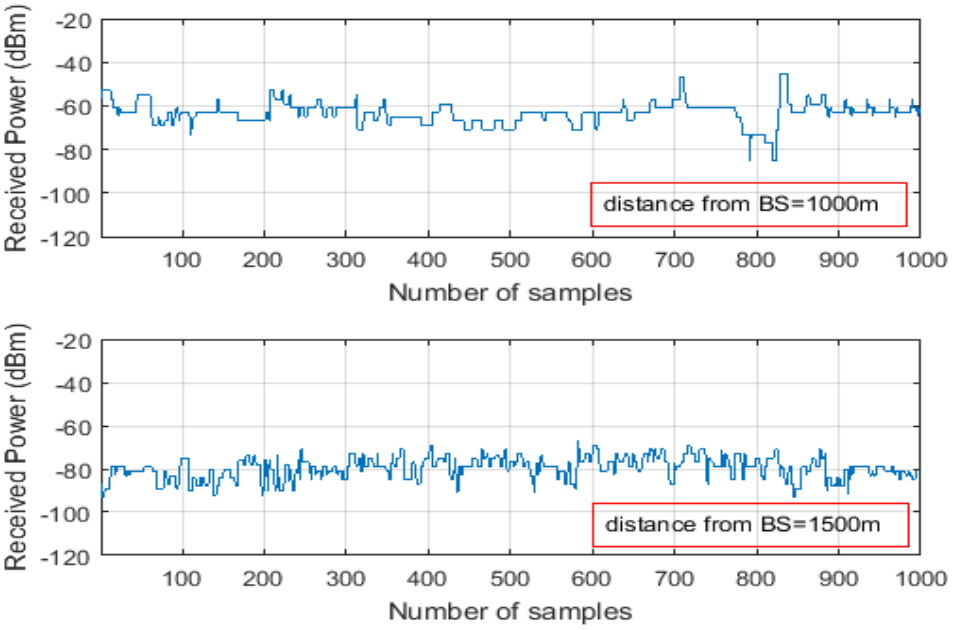

FIGURE 3.12: Measured data at 1000 and 1500 meters.

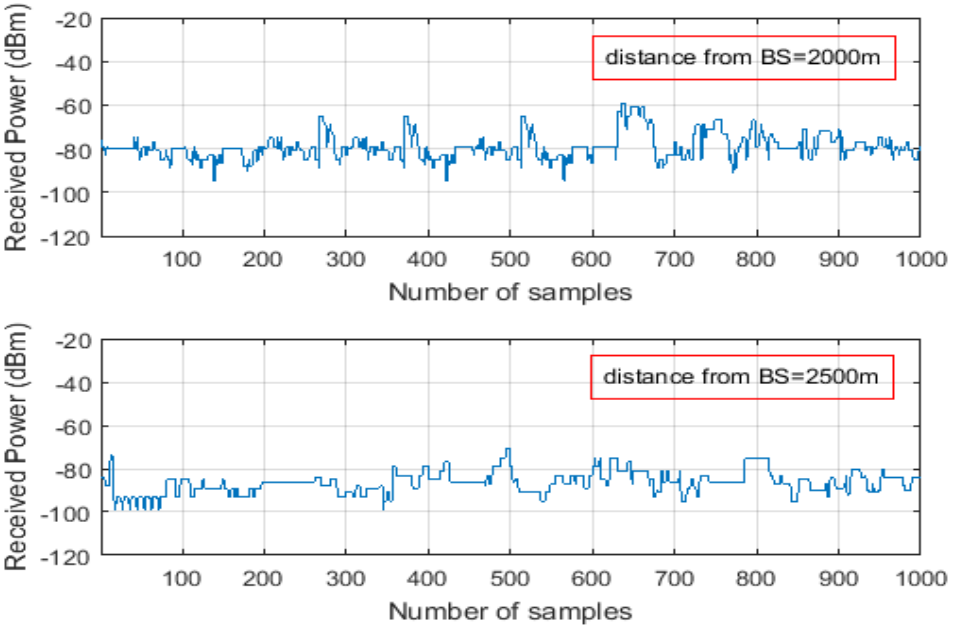

FIGURE 3.13: Measured data at 2000 and 2500 meters.

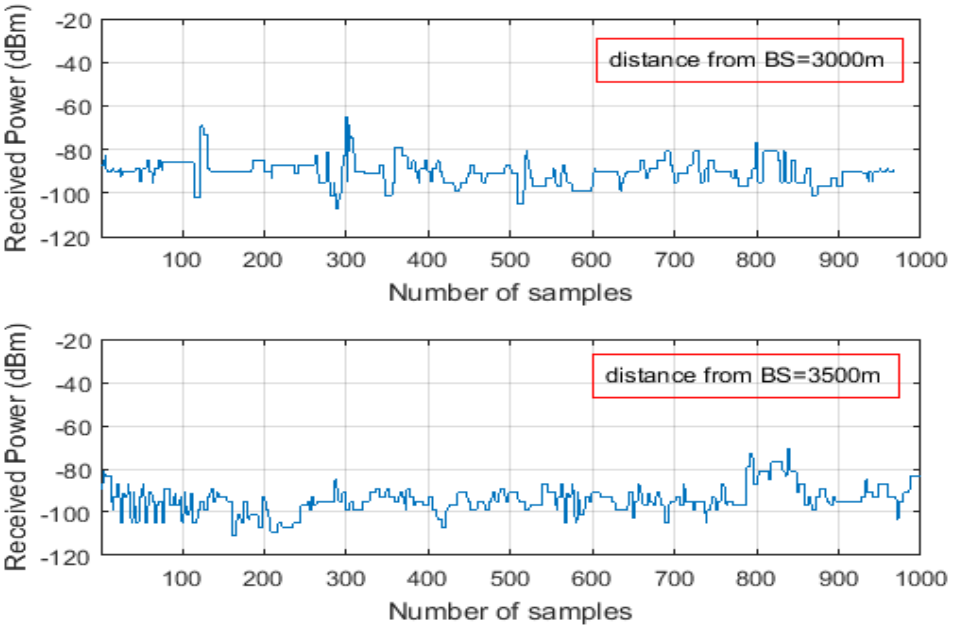

FIGURE 3.14: Measured data at 3000 and 3500 meters.

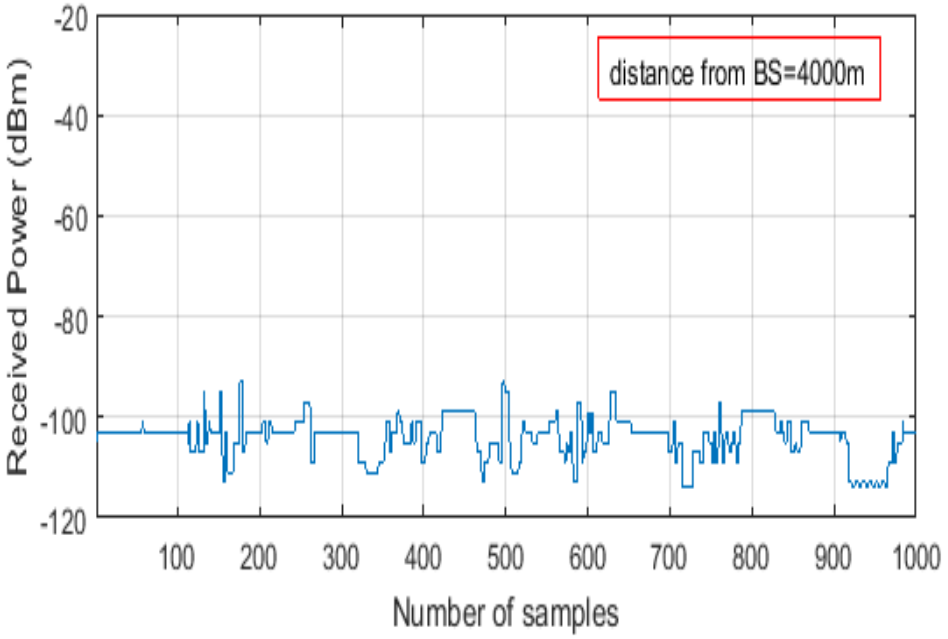

FIGURE 3.15: Measured data at 4000 meters.

Chapter 4

Comparative Analysis of Field Measurements

In this chapter, the comparison between drive test based measured pathloss and predicted pathloss using the theoretical PLMs are discussed in detail. With the help of the bar chart, the previous studies of various field measurements and their comparative analysis are also presented. By the end of this chapter, a single slope PLM is applied on the field measurements to analyze the trend of field measurements.

4.1 Comparison of Theoretical PLMs with Field Measured Data

In this research work, six predictive PLMs have been used to estimate the pathloss as discussed earlier. The detailed comparison of measured pathloss with the existing PLMs for three different BTSs: BTS1, BTS2, and BTS3 is shown in Appendix A.4 to A.6. The comparison between measured pathloss and predicted pathloss using the theoretical PLMs is graphically shown in this section.

4.1.1 Comparison of Pathloss Models with Field Measurements for BTS1

The outcome of the drive test performed in the coverage area of BTS1 resulted in a mean pathloss of 139 dB. Mean pathloss values of 127.6183 dB, 136.3034 dB, 144.9947 dB, 168.6057 dB, 122.4747 dB, 191.4006 dB are calculated by the COST-231, Hata-Okumura, Lognormal shadowing, Ericsson, SUI, and ECC- 33 PLMs respectively.

In Table 4.1, the percentage difference between the drive test based measured pathloss and predicted pathloss using the above models is presented. It is observed from Table 4.1 that the Hata-Okumura and Lognormal shadowing shows the least error of 3.36% and 2.86% respectively. Therefore, measured pathloss is best estimated by the Hata-Okumura and Lognormal shadowing PLMs among other PLMs.

TABLE 4.1: Comparison of percentage difference(error) for BTS1.

Base Station	**Hata-Okumura**	**COST-231**	**Lognormal**	**Ericsson**	**SUI**	**ECC-33**
BTS1	3.36%	9.47%	2.86%	19.23%	13.00%	34.7%

As shown in Fig 4.1, the comparison result of BTS1 shows that the ECC-33 overestimated the measured pathloss with an error of 34.7%. Because the ECC-33 model was designed for the environment of Tokyo, which is a highly build-up city. The locations used in this thesis are in urban region but not highly build-up city, therefore, ECC-33 does not show a good estimation of pathloss. However, the Hata-Okumura and Lognormal shadowing PLMs showed the closest agreement with field measurements while the SUI PLM underestimated the measured pathloss. Moreover, the COST-231 PLM shows the small variation from field measurements with an error of 9.47%.

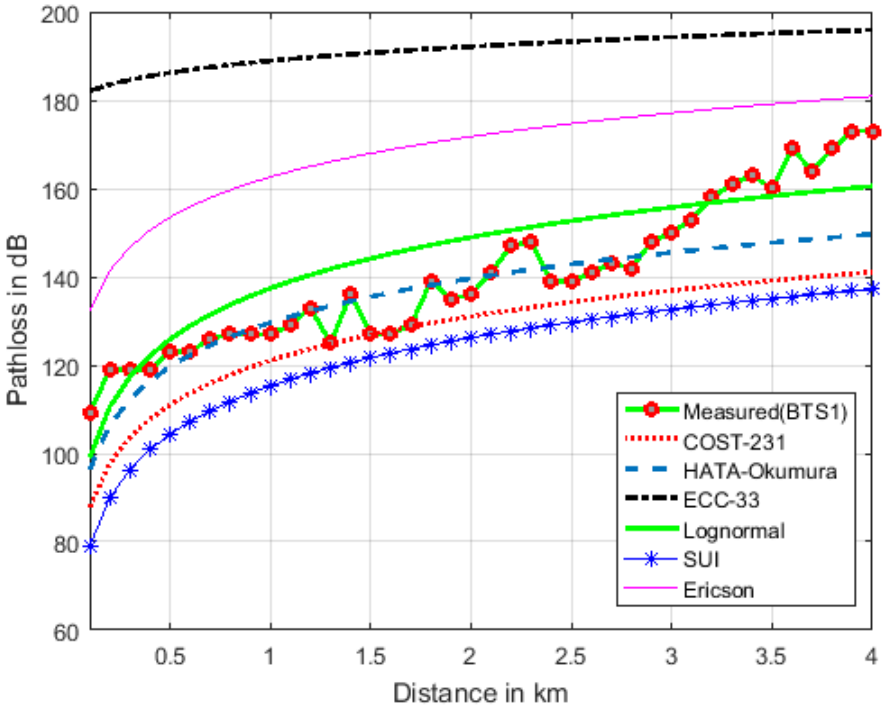

FIGURE 4.1: Comparison of estimated and field measured pathloss for BTS1.

4.1.2 Comparison of Pathloss Models with Field Measurements for BTS2

The result of the drive test performed in the coverage area of the BTS2 observed a mean pathloss of 136.55 dB. Mean pathloss values of 118.3578 dB, 126.9482 dB, 133.6706 dB, 160.1459 dB, 112.3564 dB, 215.1509 dB are predicted by the COST-231, Hata-Okumura, Lognormal Shadowing, Ericsson, SUI, and ECC-33 PLMs respectively.

In Table 4.2, the percentage difference between the measured pathloss and predicted pathloss is presented. It is clear from Table 4.2 that amongst the used PLMs, the Lognormal shadowing PLM best estimates the measured pathloss with a minimal error of 2.17%. This indicates that the measured pathloss is the best estimated by the lognormal shadowing PLM as compared to other PLMs.

From the results as depicted in Fig 4.2, it is shown that the ECC-33 and Ericson PLMs does show a quite high estimation of measured pathloss. The result of the

TABLE 4.2: Comparison of percentage difference(error) for BTS2.

Base Station	Hata-Okumura	COST-231	Lognormal	Ericsson	SUI	ECC-33
BTS2	7.26%	13.49%	2.17%	16.76%	17.78%	56.52%

ECC-33 PLM is far away from the measured pathloss that means it overestimates the measured pathloss. Moreover, the SUI PLM showed the minimum pathloss of 126.2257 dB. The Hata-Okumura model shows the small variation from field measurements with an error of 7.26%.

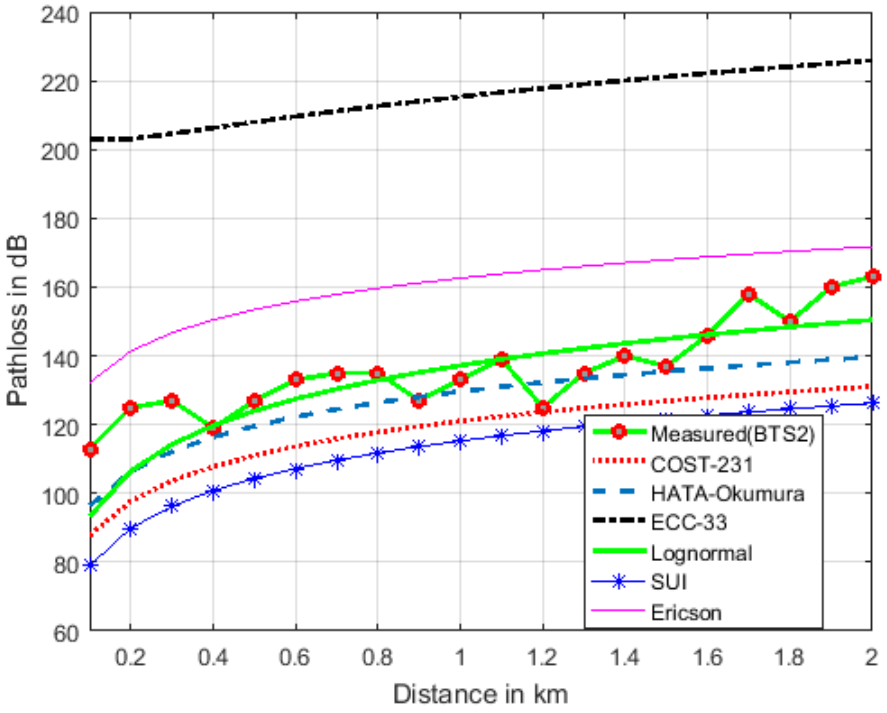

FIGURE 4.2: Comparison of estimated and field measured pathloss for BTS2.

4.1.3 Comparison of Pathloss Models with Field Measurements for BTS3

The outcome of the drive test performed in the area coverage of the BTS3 resulted in a mean pathloss of 138.55 dB. Mean pathloss values of 118.3578 dB, 126.9482 dB, 158.6706 dB, 160.1459 dB, 112.3564 dB, 284.3259 dB are predicted by the

COST-231, Hata-Okumura, Lognormal shadowing, Ericsson, SUI, and ECC-33 PLMs respectively.

In Table 4.3 shown that the Hata-Okumura PLM showed the closest agreement to the measured pathloss with a minimum error of 9.59%. This prompts that the measured pathloss is best estimated by the Hata-Okumura PLM among other PLMs. Figure 4.3 illustrates that the ECC-33 PLM showed a quite high estima-

TABLE 4.3: Comparison of percentage difference(error) for BTS3.

Base Station	**Hata-Okumura**	**COST-231**	**Lognormal**	**Ericsson**	**SUI**	**ECC-33**
BTS3	9.59%	15.64%	13.06%	13.70%	19.78%	99.10%

tion of measured pathloss of 295.1104 dB. Moreover, from distance up to 0.3 km to 1 km, the Hata-Okumura, SUI, and the COST-231 PLMs are nearer to measured pathloss while the lognormal and Ericson PLMs are nearer to the measured pathloss from distance up to 1.4 km to 2 km.

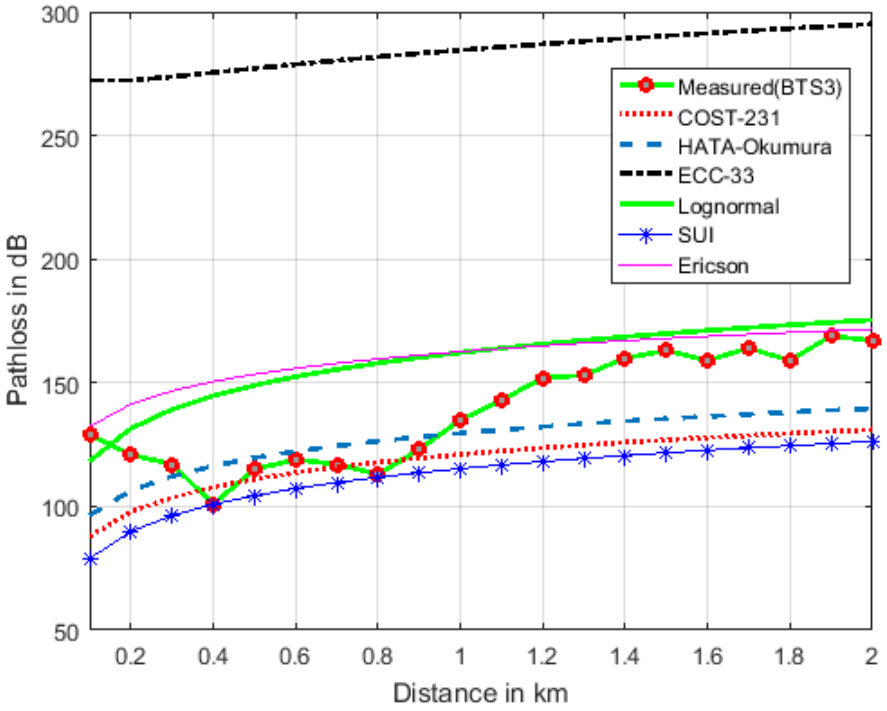

FIGURE 4.3: Comparison of estimated and field measured pathloss for BTS3.

4.2 Fitness of various Field Measurements and their Comparative Analysis

A great amount of work has been done on the comparison of field measured data with predictive PLMs in different countries [5, 6, 38, 44, 45]. Many PLMs for WCS were developed in the literature. However, selecting a suitable PLM for a given environment is not quite an easy task because terrain profile data (terrain elevation, height, clutter, altitude, and the distance between MTS and BTS) is different from place to place. For instance, several studies conducted in Malaysia, China, India, and in many other countries have indicated that the commonly used PLMs are less efficient in estimating the pathloss correctly. Fig 4.4 - 4.6 illustrates the comparison of PLMs performed in various countries along with the comparison performed in this thesis for Pakistan(2020).

As depicted in the Figs. 4.4 - 4.6, the ECC-33 PLM showed the best estimation of measured pathloss in comparative study of Tarakan, Nigeria(2018), and Tanzania. In the China Study, the COST-231 and ECC-33 PLMs are found to highly overestimate the measured pathloss while, the results of Malaysia study show that amongst the other PLMs, the SUI and lognormal shadowing PLMs showed the nearest agreement to the measured pathloss.

The outcomes of the India(2013) study show that the measured pathloss is best estimated by the SUI PLM. In Banta Algeria, India(2011) and Nigeria(2018) study, the result of the HATA-Okumura and COST-231 PLMs are found near to measured data in urban area. The results of the comparison performed in Pakistan show that the measured pathloss is best estimated by lognormal shadowing, and Hata-Okumura in all three BTSs.

Fig. 4.7 illustrates the error between the field measured pathloss and predicted pathloss obtained using theoretical pathloss models of previous studies along with the study performed in this thesis for pakistan(2020). From Fig. 4.7, it is observed that there are small variations exist between the results of this thesis and the outcomes of comparative studies performed in other countries. This is because the information about terrain is different from place to place. In this work,

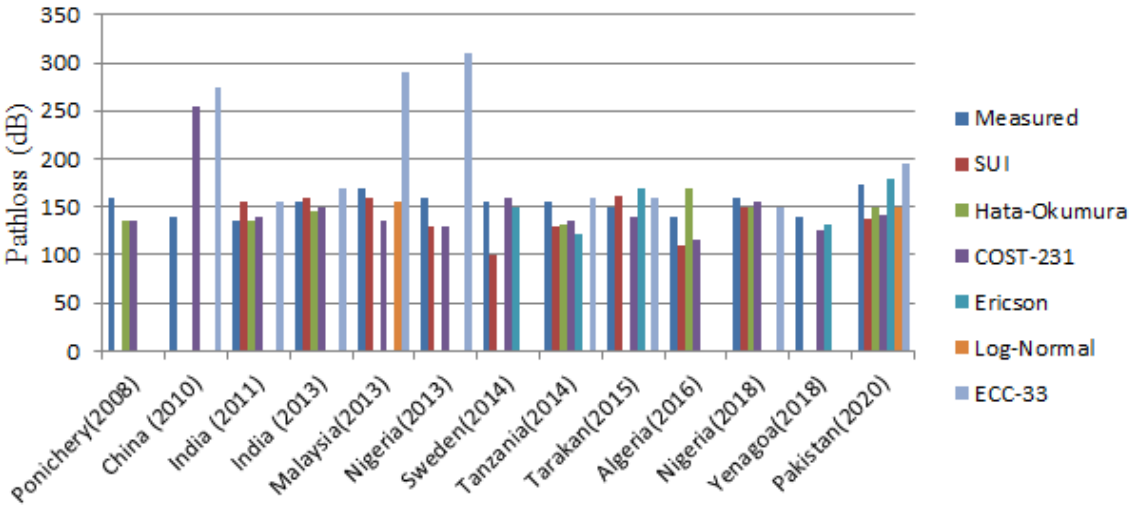

FIGURE 4.4: Fitness of field measurements of various countries with pathloss models along measurements of BTS1.

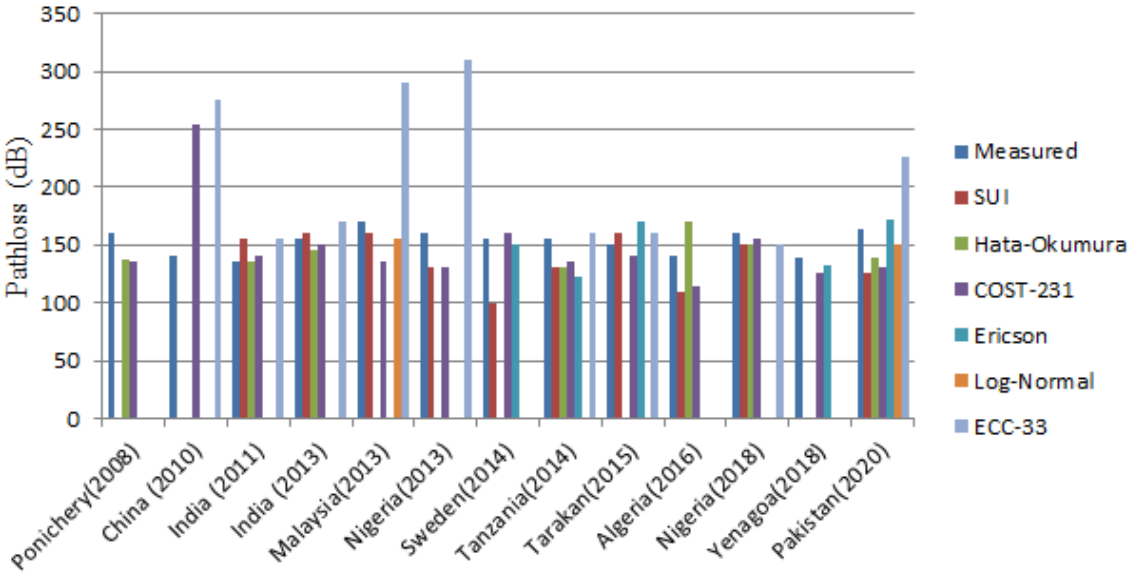

FIGURE 4.5: Fitness of field measurements of various countries with pathloss models along measurements of BTS2.

it is observed that the path loss values of the ECC-33 model are very high which means the RSS of the ECC-33 PLM is higher than the threshold level of mobile receiver -114 dBm. Hence, the ECC-33 model cannot be preferred for the maximum coverage area for the selected BTSs.

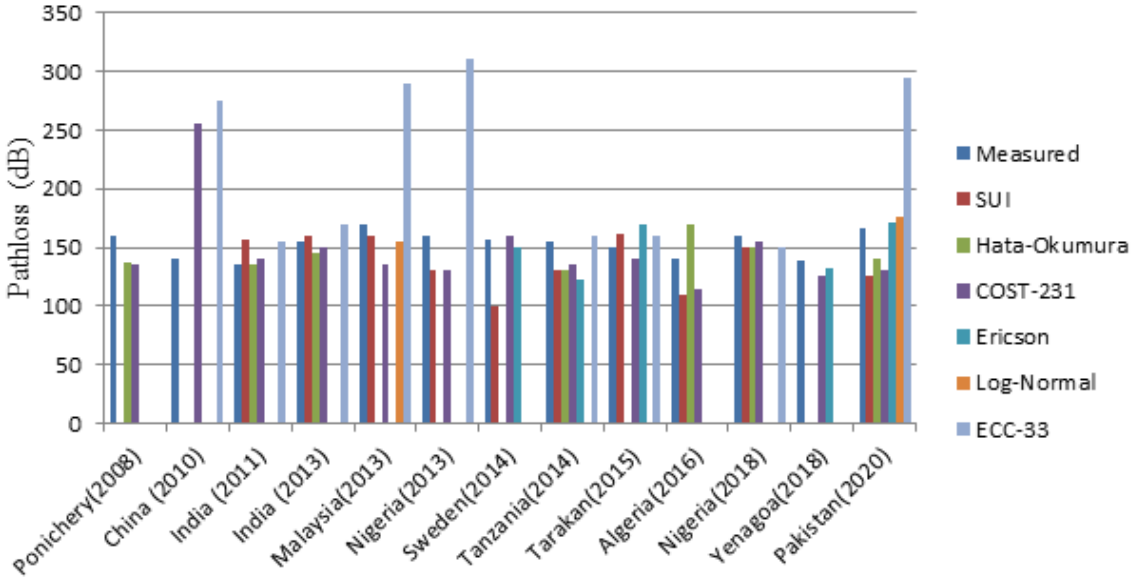

FIGURE 4.6: Fitness of field measurements of various countries with pathloss models along measurements of BTS3.

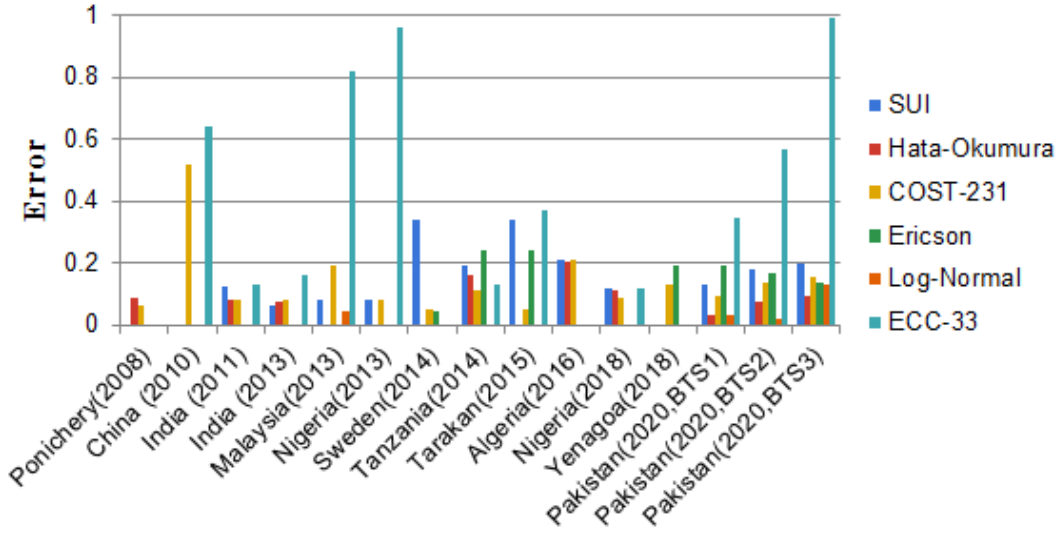

FIGURE 4.7: Error of field measurements of various countries with pathloss models along measurements of Pakistan.

4.3 Single Slope Pathloss Model

Most of the existing PLMs are of single slope, i.e., the model uses a single slope to represent the pathloss or RSS over the complete distance range. The single slope PLM is easy to analyze because it characterizes all the links distance with a single PLE. In this thesis, the single slope model is fitted on the field measurements to check whether the field measurements follow the single slope trend. From field

measurements, the average values of RSS were found to be -30 dBm and -103 dBm at a distance of 50 m and 4000 m respectively. Hence, a single slope was made by using the points: (50,-30) and (4000,-103) as shown in Fig 4.7. Afterwards, the value of slope was found by using the following equation:

$$n = \frac{Pr(d_{\min}) - Pr(d_{\max})}{10 \times \log_{10}((\frac{d_{\max}}{d_0}) - (\frac{d_{\min}}{d_0}))} \tag{4.1}$$

where, $Pr(d_{\min})$ is the RSS at the minimum distance, $Pr(d_{\max})$ is the RSS at the maximum distance, d_0 denotes the minimum distance. The difference between maximum and minimum RSS is:

$$Pr(d_{\min}) - Pr(d_{\max}) = -30dBm - (-103dBm) = 73dBm$$

The difference between maximum and minimum distance is:

$$10 \times \log_{10}(\tfrac{4000}{50} - \tfrac{50}{50}) = 18.976$$

Thus, the value of PLE is:

$$\boxed{n = \frac{73}{18.976} = 3.846}$$

As presented in Table 1.1, the above value of PLE "n" lies in the shadowed cellular urban region. The area in which the measurements were obtained is an urban region. It can be said the "shadowed urban region" because trees and vehicles became the reason for shadowing. Thus, the estimated value of PLE is correct according to the selected area as defined in [50]. In Fig 4.7. a single slope represents a trend which the measured data should follow. But, from distance 500 m to 2500 m, field measurements do not follow a single slope trend. This is due to the fact that the variations in RSS increased in that particular distance range from 500 m to 2500 m. These variations occur due to many factors including ground reflections, scattering, and shadowing, etc. Performance degradation appears because the single slope model does not capture the dependence of the PLE on the link distance correctly. This has led to the idea of multi-slope PLM, which applies different

slopes for different regions of T-R separation distances. Hence, a multi-slope model is used in the next chapter to overcome this problem.

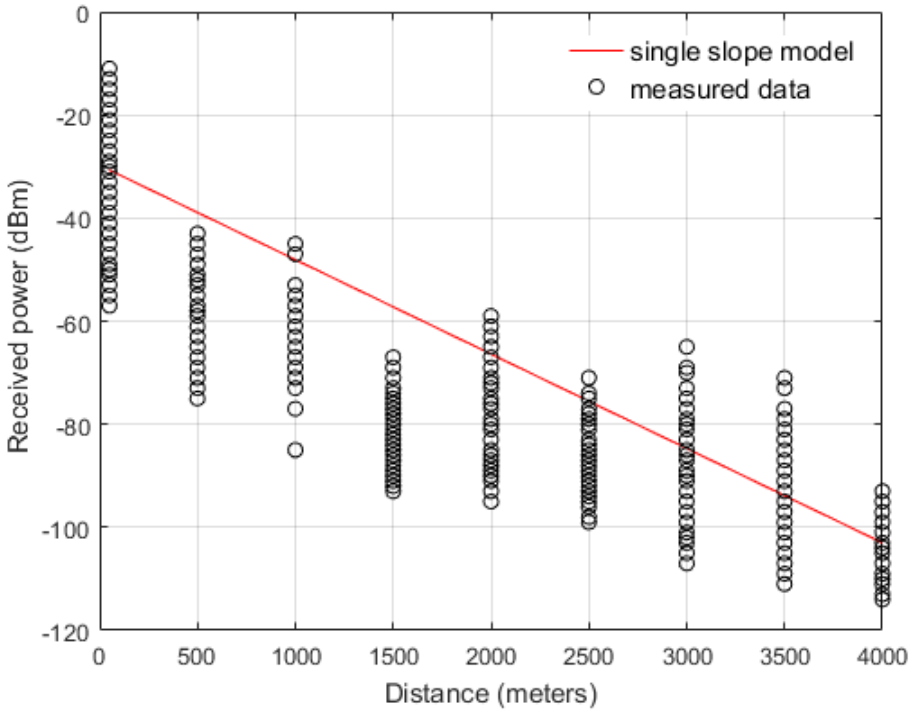

FIGURE 4.8: Single slope pathloss model.

Chapter 5

Multi-slope Lognormal Shadowing Pathloss Model

The single-slope PLM mostly falls short in precisely capturing the PLE dependence on the physical propagation environment. This limitation leads to the consideration of multi-slope PLM, which is discussed in this chapter. The multi-slope PLM has been presented in two different ways namely, segmental multi-slope PLM and single-reference multi-slope PLM. A comparison of these two multi-slope PLMs is also mentioned. Furthermore, the lognormal shadowing PLM is evaluated using a segmental multi-slope model. At the end of this chapter, the distribution of field measurements at various distances are discussed in detail.

5.1 The Modified Multi-slope Pathloss Model

Practically, propagation is very difficult to characterize due to multipath fading, ground reflections, shadowing, scattering, and many other physical conditions. Since the number of possible realizations of physical propagation environments is boundless, a single slope PLM mostly falls short in precisely capturing the physical propagation environment. The single slope model characterizes all the links with a single PLE. The densification of wireless network causes more uncertainties in cell

patterns and thus, the communication links cannot be accurately estimated by a single PLE [58, 59]. Therefore, the multi-slope PLM is more realistic to estimate the increased variations in the communication links.

Multi-slope PLM involves different PLEs for various link distances. The value of PLE determines the signal decay rate in each distance range [36, 37]. In this thesis, the field measurements is modeled using multi-slope modeling with six different segments as shown in Fig 5.1.t

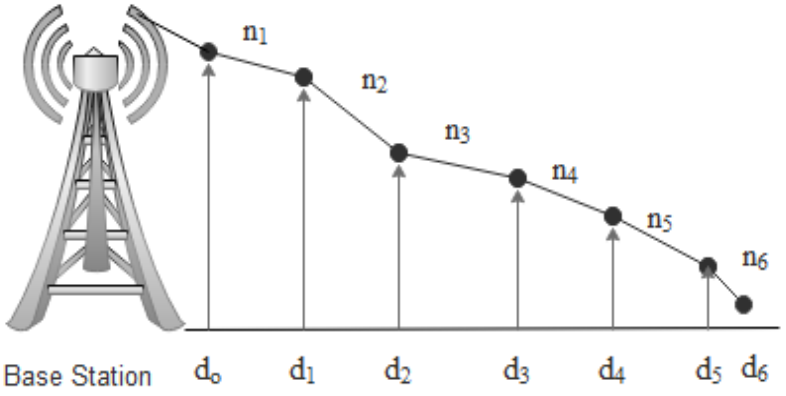

FIGURE 5.1: Multi-slope model.

In Fig 5.1, the n_1, n_2, n_3, n_4, n_5, and n_6 represent the values of slopes of segments: d_0 to d_1, d_1 to d_2, d_2 to d_3, d_3 to d_4, d_4 to d_5, and d_5 to d_6 respectively. Multi-slope PLM can be divided into two types; i.e. Segmental multi-slope PLM [56, 57] and Single-reference multi-slope PLM.

5.1.1 Segmental Multi-slope Pathloss Model

The segmental multi-slope PLM involves multiple segments with different PLEs. This model considers various slopes above and beyond the breakpoint distance. The breakpoint distance is the distance where the slope changes [60, 61]. In this thesis, the segmental multi-slope PLM has six slopes as shown in Fig 5.2. The values of the PLE of each segment are calculated. The following formula is used

to develop a segmental multi-slope PLM:

$$P(d_1) = P_0(\frac{d_0}{d_1})^{n_1} \tag{5.1}$$

where, $P(d_1)$ denotes the RSS at a distance d_1, P_0 represents the RSS at a refrence distance(d_0) from transmitter and n_1 represents the value of slope from d_0 to d_1 segment as shown in Fig 5.1. Likewise, the received power for segment-2, segment-3, and segment-4 are presented by the following equations:

$$P(d_2) = P_0(\frac{d_1}{d_2})^{n_2} \tag{5.2}$$

$$P(d_3) = P_0(\frac{d_2}{d_3})^{n_3} \tag{5.3}$$

$$P(d_4) = P_0(\frac{d_3}{d_4})^{n_4} \tag{5.4}$$

$$P_4 = P_0(\frac{d_0}{d_1})^{n_1}(\frac{d_1}{d_2})^{n_2}(\frac{d_2}{d_3})^{n_3}(\frac{d_3}{d_4})^{n_4} \tag{5.5}$$

The received power in each segment is sensitive to equation 5.1, 5.2, 5.3, and 5.4. In this thesis, six different segments are proposed. Hence, the equation for the six segments will be:

$$P_6 = P_0(\frac{d_0}{d_1})^{n_1}(\frac{d_1}{d_2})^{n_2}(\frac{d_2}{d_3})^{n_3}(\frac{d_3}{d_4})^{n_4}(\frac{d_4}{d_5})^{n_5}(\frac{d_5}{d_6})^{n_6} \tag{5.6}$$

For generalization,

$$P_{\mathrm{N}} = P_0(\frac{{d_0}^{n_1}}{{d_1}^{n_1}} \times \frac{{d_1}^{n_2}}{{d_2}^{n_2}} \times \frac{{d_2}^{n_3}}{{d_3}^{n_3}} \times \frac{{d_3}^{n_4}}{{d_4}^{n_4}} \times \frac{{d_4}^{n_5}}{{d_5}^{n_5}} \times \frac{{d_5}^{n_6}}{{d_6}^{n_6}}) \tag{5.7}$$

$$P_{\mathrm{N}} = P_0({d_0}^{n_1}{d_1}^{n_2-n_1} \times {d_2}^{n_3-n_2}{d_3}^{n_4-n_3} \times {d_4}^{n_5-n_4}{d_5}^{n_6-n_5} \times {d_6}^{-n_6}) \tag{5.8}$$

Thus, the following formula of segmental multi-slope PLM is used for calculating the value of PLE for each segment,

$$\boxed{P_{\mathrm{N}} = \prod_{i=1}^{N} P_0(\frac{d_{\mathrm{i}-1}}{d_{\mathrm{i}}})^{n_{\mathrm{i}}}} \tag{5.9}$$

Fig 5.2 below illustrates the slope is divided into six different segments, therefore it is known as segmental multi-slope PLM. In order to model the measured data properly, the segments are made according to the field measurements. The x-axis shows the distance from 50 to 4000 m in the logarithmic scale and the y-axis shows the RSS in dBm. The values of PLE "n" are found for every segment using field measurements. To estimate the RSS, PLE is an important factor in wireless communication. The average values of RSS at various distances are plotted against distance. The measured data is fitted on the average values at a distance of 50 m, 500 m, 1000 m, 1500 m, 2000 m, 3000 m, and 4000 m. From the results

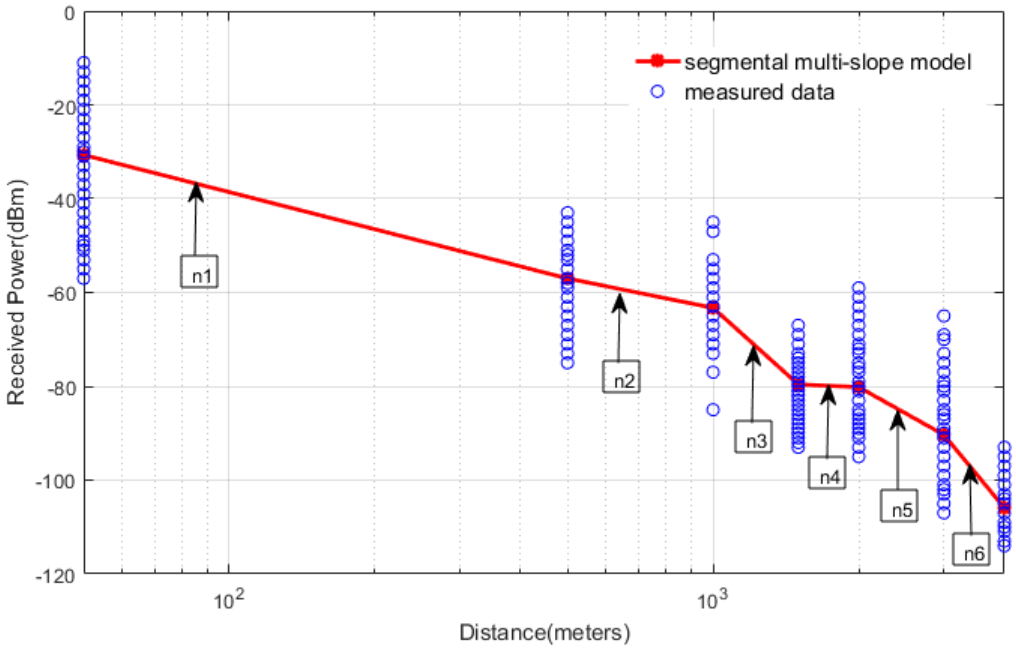

FIGURE 5.2: Segmental multi-slope pathloss model with different PLEs.

shown in Table 5.1, it is observed that the signal decay rate is high in segments n_3, and n_6 which means the rate of decreasing RSS is higher than as compared to other segments. This is due to the obstacles such as, trees, buildings, and trucks which cause the shadowing effects and then data deviated from the mean value. The value of n_4 is very small that means the decreasing rate of RSS is very low. When the value of n <2 means that for short distances, the effects of path loss are fairly negligible versus for example the positive impact of reflections or directionality [57]. The variation in PLE relies on the value of RSS, that is, whenever there is a speedy fall in the values of RSS, the PLE is increased.

TABLE 5.1: Parameters of segmental multi-slope pathloss model.

Segments	**Distance(m)**	**Break point(m)**	**PLE** n
n_1	50-500	500	2.632
n_1	500-1000	1000	2.190
n_3	1000-1500	1500	9.26
n_4	1500-2000	2000	0.456
n_5	2000-3000	3000	5.78
n_6	3000-4000	4000	10.85

5.1.2 Single-Reference Multi-slope Pathloss Model

In this section, multi-slope PLM is implemented by keeping the same reference distance d_0 in all segments as shown in Table 5.2. It would be clear more by the following formula which has been used in simulating the multi-slope PLM with respect to reference distance:

$$\boxed{P(d_{\mathrm{N}}) = \prod_{i=1}^{N} P_0(\frac{d_0}{d_{\mathrm{i}}})^{n_{\mathrm{i}}}} \tag{5.10}$$

where, d_0 represents the reference distance, d_{i} is the changing distance from one segment to another, P_0 is the RSS at d_0, N represents the total number of segments and here the value of N is six. As shown in Fig 5.3, n_1, n_2, n_3, n_4, n_5, and n_6 represent the signal decay rate of each segment. The slope of each segment is started from a single point because here, d_0 is considered constant in all segments but d_{i} changes when we move towards the next segment. From the results of Table 5.2, it can be noticed that the values of PLE are gradually increased in the single-reference multi-slope PLM. This is because as the MTS moves away from the BTS, the signal decay rate increases with the transmission distance so the corresponding PLE is increased. The single-reference multi-slope PLM is showing the best estimation of PLE as compared to segmental multi-slope model.

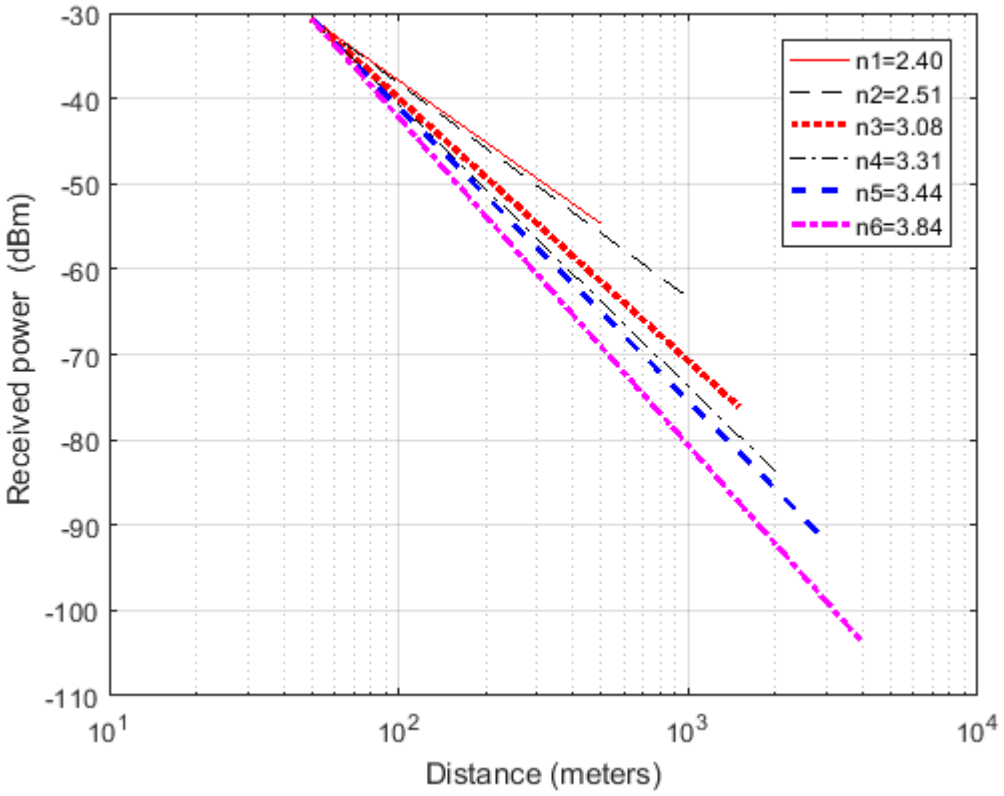

FIGURE 5.3: Multi-slope pathloss model with respect to reference distance.

TABLE 5.2: Values of PLE.

Distance(m)	**Break point position(m)**	**PLE** n
50-500	500	2.40
50-1000	1000	2.51
50-1500	1500	3.08
50-2000	2000	3.31
50-3000	3000	3.44
50-4000	4000	3.84

5.2 Comparison of Multi-slope Pathloss Models

In this section, the values of PLE which have been estimated using two different modified multi-slope PLMs are compared with each other. The estimation of PLE has been performed using the following two cases:

- Case 1: Segmental multi-slope PLM.
- Case 2: Single-reference multi-slope PLM.

In Table 5.3, it is shown that the values of PLE are different in both cases. When the environment gets worse due to ground reflections, scattering, shadowing, and other physical features cause the measured PLE increase in some segments, the decreasing rate of RSS is higher than the other segments and due to this, the corresponding PLEs are also higher.

It is clear from Table 5.3 that the PLE increases gradually in case-2 whereas the values of PLE aren't increased gradually in case-1. The n_3 and n_6 of case-1 is quite higher than the case-2 which means the signal decay rate is high in that particular segments of case-1 as compared to case-2. This is due to the existing obstacles such as, trees, buildings, or trucks which increases the effect of shadowing and causes the n_3 and n_6 of case-1 increased. On the other side, n_4 of case-1 is very small as compared to case-2, which means the decreasing rate of RSS is very low. In case-2, the values of PLE are smaller than the PLEs of case-1 except for the value of n_2. Since case-2 showed a gradual trend of PLEs in which the values of PLE is gradually increased, therefore, the case-2 (single-reference multi-slope PLM) can be preferred over case-1 (segmental multi-slope PLM) theoretically. But practically, the segmental multi-slope PLM is more realistic to approximate the increased variations in the links.

5.3 The Proposed Multi-slope Lognormal Shadowing Pathloss Model

In wireless networks, theoretical PLMs are largely based on single slope PLM, which falls short in accurately capturing the fading effects of the physical propagation environment. However the analysis of the measurement data does not show agreement with this practice and reflects a multi-slope behavior. The impact of

TABLE 5.3: Comparison of segmental and single-reference multi-slope pathloss models on the basis of PLE.

PLE	**Segments in Case-1**	**Case-1**	**Segments in Case-2**	**Case-2**
n_1	50-500	2.632	50-500	2.40
n_2	500-1000	2.190	50-1000	2.51
n_3	1000-1500	9.261	50-1500	3.08
n_4	1500-2000	0.456	50-2000	3.31
n_5	2000-3000	5.78	50-3000	3.44
n_6	3000-4000	10.85	50-4000	3.84

the multi-slope phenomenon is evident from the variation in the PLE of different segments of Islamabad Expressway. The lognormal shadowing PLM is thus chosen based on its smallest error with the measured pathloss data and is further extended to multi-slope lognormal shadowing PLM. RSS usually varies due to the shadowing effect and shadowing is generated due to various hurdles between BTS and MTS. Hence, the lognormal shadowing model is used to characterize the shadowing effect. The shadowing effects have been modeled with multiple slopes by using the equation 5.7.

$$P_{\mathrm{N}} = P_0\left(\frac{{d_0}^{n_1}}{{d_1}^{n_1}} \times \frac{{d_1}^{n_2}}{{d_2}^{n_2}} \times \frac{{d_2}^{n_3}}{{d_3}^{n_3}} \times \frac{{d_3}^{n_4}}{{d_4}^{n_4}} \times \frac{{d_4}^{n_5}}{{d_5}^{n_5}} \times \frac{{d_5}^{n_6}}{{d_6}^{n_6}}\right) \tag{5.11}$$

By taking log on the right side of equation, the equation (5.11) can be rewritten as:

$$\begin{aligned} P_{\mathrm{N}} = P_0 &- 10n_1\log\left(\frac{d_0}{d_1}\right) - 10n_2\log\left(\frac{d_1}{d_2}\right) - 10n_3\log\left(\frac{d_2}{d_3}\right) - 10n_4\log\left(\frac{d_3}{d_4}\right) \\ &- 10n_5\log\left(\frac{d_4}{d_5}\right) - 10n_6\log\left(\frac{d_5}{d_6}\right) \end{aligned} \tag{5.12}$$

It is important to note that (5.12) gives the received power as a function of segment PLEs and distances only and there is no consideration of environmental clutter in it. Therefore, to account for the possible variation in received power due to

numerous environmental factors, we add shadowing factor $X_{\sigma_{\mathrm{N}}}$ in (5.12) to get:

$$\begin{aligned} P_{\mathrm{N}} = P_0 - 10n_1 \log(\frac{d_0}{d_1}) - 10n_2 \log(\frac{d_1}{d_2}) - 10n_3 \log(\frac{d_2}{d_3}) - 10n_4 \log(\frac{d_3}{d_4}) \\ - 10n_5 \log(\frac{d_4}{d_5}) - 10n_6 \log(\frac{d_5}{d_6}) + X_{\sigma_{\mathrm{N}}} \end{aligned} \tag{5.13}$$

Here, the following assumption is made,

$$(\frac{d_0}{d_1}) = (\frac{d_1}{d_2}) = (\frac{d_2}{d_3}) = (\frac{d_3}{d_4}) = (\frac{d_4}{d_5}) = (\frac{d_5}{d_6}) = \alpha \tag{5.14}$$

where $\alpha > 1$, hence the equation (5.13) can be rewritten as:

$$\begin{aligned} P_{\mathrm{N}} = P_0 - 10n_1 \log(\alpha) - 10n_2 \log(\alpha) - 10n_3 \log(\alpha) - 10n_4 \log(\alpha) - 10n_5 \\ \log(\alpha) - 10n_6 \log(\alpha) + X_{\sigma_{\mathrm{N}}} \end{aligned} \tag{5.15}$$

By taking the $\log(\alpha)$ common from equation (5.15) to get:

$$P_{\mathrm{N}} = P_0 - 10 \log(\alpha)[n_1 + n_2 + n_3 + n_4 + n_5 + n_6] + X_{\sigma_{\mathrm{N}}} \tag{5.16}$$

The N-slope lognormal shadowing PLM can be defined as:

$$\boxed{P_{\mathrm{N}} = P_0 - 10\tilde{n} \log(\alpha) + X_{\sigma_{\mathrm{N}}}} \tag{5.17}$$

where, $\tilde{n}$ represents the sum of all PLEs, $X_{\sigma_{\mathrm{N}}}$ denotes the standard deviation of six segments, and $Pr(d_0)$ represents the received power at close-in reference distance. In this thesis, channel parameters are modeled in each segment with the different PLEs n and standard deviation, σ. Fig 5.4 shows the proposed segmental multi-slope lognormal shadowing PLM for an outdoor area. The values of PLE n and σ were calculated by utilizing the measured data gathered during the site surveys. The dotted lines show the upper and lower boundaries of 4σ in Fig 5.4. The upper boundary of σ is not significant to this model because the upper limit does not have any negative effect on the system. From this graph, it can be observed that all the data points fall within the fourth standard deviation, 4σ, from the mean, μ.

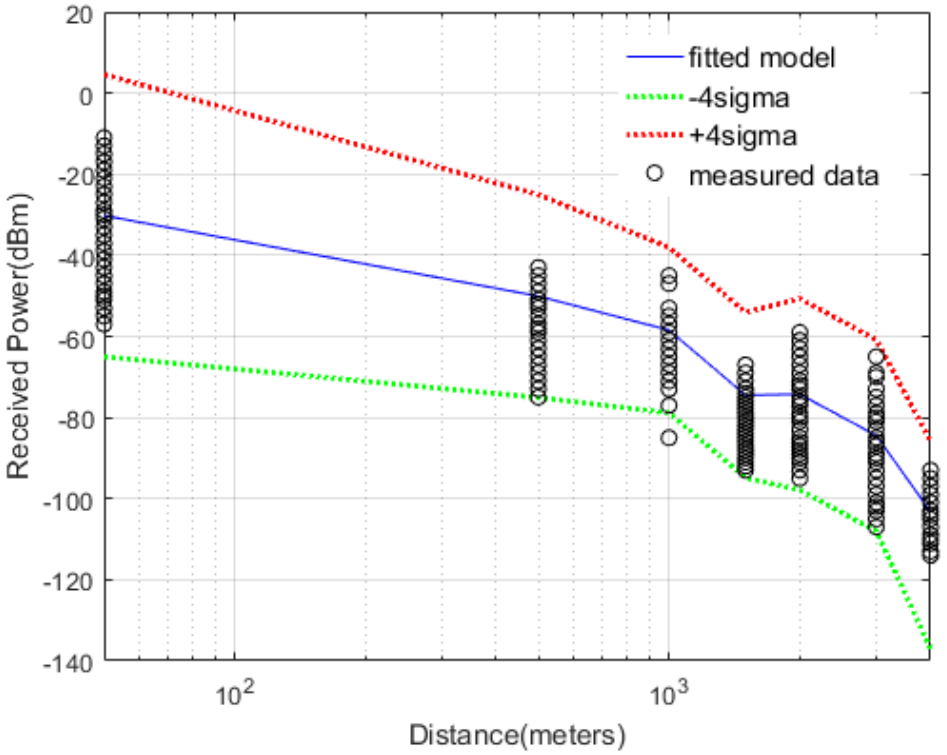

FIGURE 5.4: Proposed segmental multi-slope lognormal shadowing pathloss model.

To optimize and validate the effectiveness of the proposed model, the error is calculated between the results of the proposed model and the single slope lognormal shadowing PLM for BTS1. The optimization is a process in which the lognormal shadowing PLM is adjusted using a segmental multi-slope model. The aim is to get the predicted pathloss as close as possible to the measured pathloss. From the result as depicted in Fig 5.4, it is shown that the multi-slope lognormal shadowing PLM does show a good agreement to the field measurements. This model best fitted on the field measurements using the multi-slope model. Hence, the proposed model showed the best estimation and can estimate the field measured data with a minimal error of 2.15% compared to single slope lognormal shadowing PLM was about 2.86% as shown in Fig 5.5.

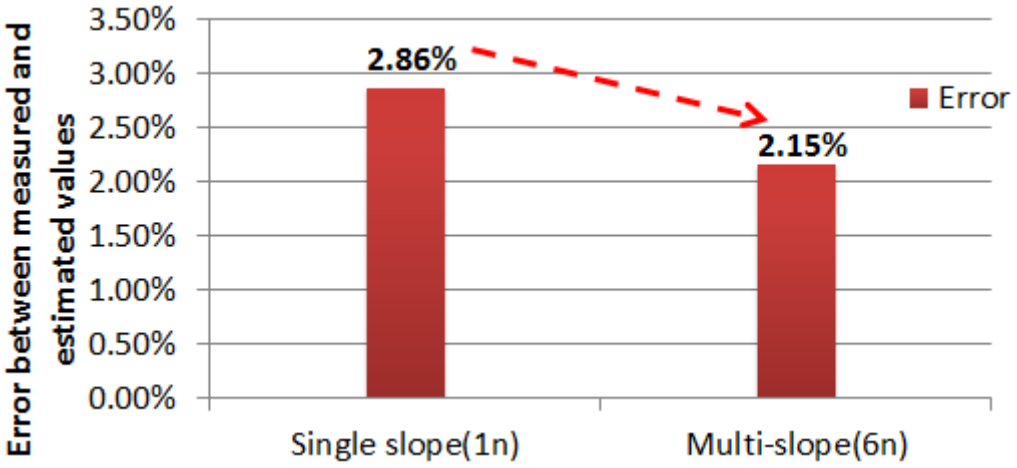

FIGURE 5.5: Error of single slope and multi-slope lognormal shadowing pathloss model.

5.4 Distribution of Field Measurements at various Distances

In order to analyze the performance of cellular networks over different conditions (shadowing, multipath fading, ground reflections, scattering, etc.), the propagation channel is modeled as a lognormal distribution. Firstly, needs to estimate the parameters (μ and σ) of the lognormal distribution in real environments from field measurements. In this regard, the probability density functions (PDFs) of lognormal distribution are plotted at distances of 50 m, 1000 m, 1500 m, 2000 m, 2500 m, 3000 m, 3500 m, 4000 m as shown in Fig 5.5 to 5.13 (see Appendix B). The curves of the PDFs corresponding to the lognormal distribution generated by using the distribution fitting tool in MATLAB.

From the results as depicted in Fig 5.5 - 5.13, it is shown that the distribution of field measurements of each location is a lognormal distribution with different distribution parameters as shown in Table 5.4. In lognormal distribution, 68% of the measured data should fall in one standard deviation, 1σ, and 95% of the measured data should fall in 2σ [50]. From results, it is observed that more than 90% of measured data fall in two standard deviation, 2σ. This is closed to the theoretical results as discussed earlier. Therefore we can still say that this

lognormal model comes out to be accurate because approximately measured data of each location fall in the two standard deviation, 2σ.

TABLE 5.4: Parameters of lognormal distribution.

Distances (m)	**Mean**	**Sigma**	**Data in -2σ to $+2\sigma$**	**Data in 2σ to $+3\sigma$**
50	92.6	8.7	91%	4.8%
500	119.0	6.25	90%	3.6%
1000	125.2	5.13	94%	3.9%
1500	141.6	5.1	93%	7.4%
2000	141.1	5.9	94%	5.3%
2500	148.4	4.9	86%	13%
3000	152.3	5.9	89%	5.9%
3500	156.2	6.6	96%	3.4%
4000	166.0	3.7	93%	3.3%

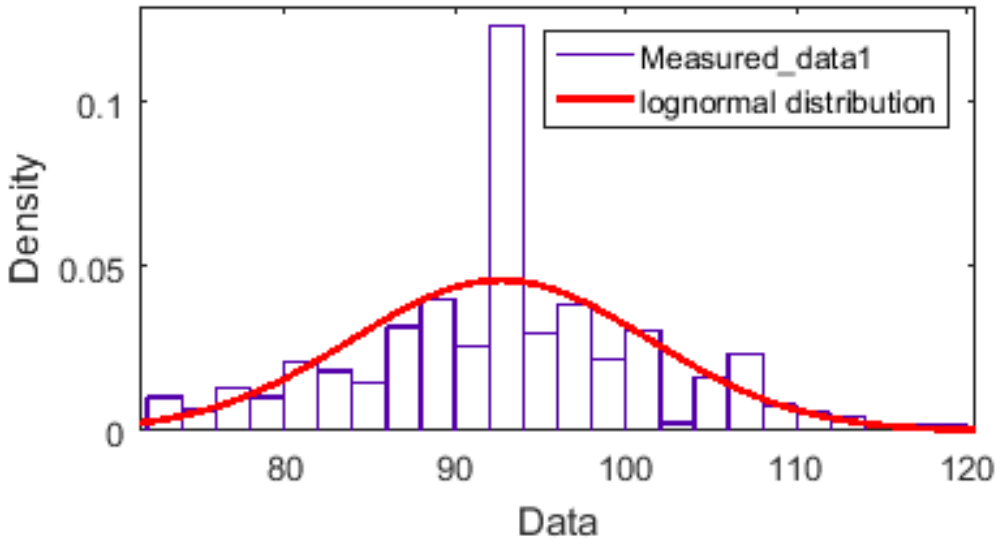

FIGURE 5.6: Distribution of measured data at distance of 50m.

Chapter 6

Conclusion and Future Work

In this thesis, we have provided a comparison of six theoretical PLMs, i.e., Hata-Okumura, ECC-33, Ericson, SUI, Lognormal shadowing, and COST-231 with field measurements. The comparison has been performed in three different locations: Koral Town, Korang Town and Soan Garden situated on Islamabad Expressway, Pakistan. Furthermore, the multi-slope model has been used to improve the performance of single slope PLMs.

6.1 Conclusion

After analyzing the results obtained through simulation of both comparative analysis of PLMs and multi-slope PLMs, this entire work is concluded in the subsequent paragraphs as follows;

The measured pathloss, when compared with theoretical values based on percentage difference, the lognormal shadowing PLM showed the closest agreement to the measured pathloss with a minimum error of 2.86% and 2.17% for BTS1 and BTS2 respectively. The measured pathloss in BTS3 is best estimated by the Hata-Okumura PLM with an error of 9.59%. The ECC-33 PLM overestimates the measured pathloss of BTS1, BTS2, and BTS3 with a maximum error of 34%, 56%, and 99% respectively. Hence, the ECC-33 model cannot be preferred for the

coverage area of the selected BTSs.

This thesis also studied the multi-slope PLM, where different link distances are characterized by different PLEs. The analysis of the single slope model was not shown the closest agreement to the field measurement data. Based on the results of a single slope PLM, a multi-slope model has been used in two different ways named as a segmental multi-slope model and single-reference multi-slope model. For performance analysis, the simulations of both multi-slope models have been performed in MATLAB. It has been observed from the results that the single-reference multi-slope model showed a good estimation of PLE in comparison to the segmental multi-slope model.

Single slope lognormal shadowing PLM showed the closest agreement to the measured pathloss in terms of its error. Based on this, a lognormal shadowing PLM has been further extended to multi-slope lognormal shadowing PLM. The proposed lognormal shadowing PLM model showed high accuracy and making the minimum error to 2.15% as compared to the single slope lognormal shadowing PLM was about 2.86%. Furthermore, the distribution of field measurements at various distances are also analyzed using lognormal distribution. It has been extracted from the results that more than 90% measured data fall in 2σ. Therefore, this lognormal model comes out to be accurate because approximately measured data fall within 2σ.

6.2 Future Work

The work performed in this thesis provides a base for several future works. Collected field measurements can be used to analyze the effect of the pathloss in different applications that depend on RSS and PLE like RSS-based localization. In future, the use of multi-slope model can be extended with different pathloss models. Moreover, the pathloss models can be implemented by using different machine learning techniques to estimate the pathloss.

Appendix A

Distance-wise Comparison of Propagation Models with Field Measurements

The values of the RSS were taken at an interval of 0.1 km as shown in Table A.1 to A.3. The hundred measurements are taken at distances of 0.1 km, 0.2 km, 0.3 km up to 4km, 2km and 2km for BTS1, BTS2, and BTS3 respectively. By utilizing the field measurements, the pathloss is measured. The comparison of measured pathloss with the existing PLMs for three different BTSs: BTS1, BTS2, and BTS3 is shown in Appendix A.4 to A.6.

TABLE A.1: Measured pathloss and RSS from BTS1 located in Koral town.

Distance(km)	**RSS(dBm)**	**Measured Pathloss(dB)**
0.1	-47	109
0.2	-57	119
0.3	-57	190
0.4	-57	119
0.5	-61	123
0.6	-61	123
0.7	-64	126
0.8	-65	127
0.9	-65	127
1.0	-65	127
1.1	-67	129
1.2	-71	133
1.3	-63	125
1.4	-74	136
1.5	-65	127
1.6	-65	127
1.7	-67	129
1.8	-77	139
1.9	-73	135
2.0	-74	136
2.1	-79	141
2.2	-85	147
2.3	-86	148
2.4	-77	139
2.5	-77	139
2.6	-79	141
2.7	-81	143
2.8	-80	142
2.9	-86	148
3.0	-88	150
3.1	-91	153
3.2	-96	158
3.3	-99	161
3.4	-101	163
3.5	-98	160
3.6	-107	169
3.7	-102	164
3.8	-107	169
3.9	-111	173
4.0	-111	173

TABLE A.2: Measured pathloss and RSS from BTS2 located in Korang town.

Distance(km)	**RSS(dBm)**	**Measured Pathloss(dB)**
0.1	-51	113
0.2	-63	125
0.3	-65	127
0.4	-57	119
0.5	-65	127
0.6	-71	133
0.7	-73	135
0.8	-73	135
0.9	-65	127
1.0	-71	133
1.1	-77	139
1.2	-63	125
1.3	-73	135
1.4	-78	140
1.5	-75	137
1.6	-84	146
1.7	-96	158
1.8	-92	154
1.9	-98	160
2.0	-101	163

TABLE A.3: Measured pathloss and RSS from BTS3 located in Soan garden.

Distance(km)	**RSS(dBm)**	**Measured Pathloss(dB)**
0.1	-67	129
0.2	-59	121
0.3	-55	117
0.4	-39	101
0.5	-53	115
0.6	-57	119
0.7	-55	117
0.8	-51	113
0.9	-61	123
1.0	-73	135
1.1	-81	143
1.2	-90	152
1.3	-91	153
1.4	-98	160
1.5	-101	163
1.6	-97	159
1.7	-102	164
1.8	-97	159
1.9	-107	169
2.0	-105	167

TABLE A.4: Comparison of estimated values of pathloss models with field measurements from BTS1 located in Koral town.

Distance(km)	Measured Pathloss(dB)	Hata-Okumura (dB)	COST-231 (dB)	Lognormal (dB)	Ericson(dB)	SUI (dB)	ECC-33 (dB)
0.1	109	96.3784	87.7880	98.9996	132.2194	78.9549	182.1149
0.2	119	106.3886	97.7982	110.5591	141.3640	89.8924	183.5230
0.3	119	112.2442	103.6538	117.3210	146.7133	96.2903	184.6015
0.4	119	116.3988	107.8084	122.1187	150.5087	100.8298	185.4807
0.5	123	119.6213	111.0309	125.8400	153.4526	104.3509	186.2279
0.6	123	122.2543	113.6640	128.8806	155.8579	107.2278	186.8807
0.7	126	124.4805	115.8901	131.4513	157.8916	109.660	187.4623
0.8	127	126.4089	117.8186	133.6782	159.6533	111.7672	187.9881
0.9	127	128.1099	119.5195	135.6425	161.2072	113.6258	188.4688
1.0	127	129.6315	121.0411	137.3996	162.5972	115.2883	188.9122
1.1	129	131.0079	122.4176	138.9890	163.8546	116.7922	189.3243
1.2	133	132.2645	123.6741	140.4401	165.0026	118.1652	189.7096
1.3	125	133.4205	124.8301	141.7750	166.0586	119.4282	190.0717
1.4	136	134.4907	125.9003	143.0109	167.0363	120.5976	190.4134
1.5	127	135.4871	126.8967	144.1615	167.9465	121.6863	190.7372
1.6	127	136.4191	127.8287	145.2378	168.7979	122.7046	191.0451
1.7	129	137.2946	128.7043	146.2488	169.5978	123.6613	191.3386
1.8	139	138.1201	129.5297	147.2020	170.3518	124.5632	191.6192
1.9	135	138.9009	130.3105	148.1037	171.0652	125.4163	191.8880
2.0	136	139.6417	131.0513	148.9591	171.7419	126.2257	192.1462
2.1	141	140.3463	131.7559	149.7728	172.3855	126.9956	192.3945
2.2	147	141.0181	132.4277	150.5486	172.9993	127.7296	192.6338
2.3	148	141.6601	133.0697	151.2899	173.5857	128.4311	192.8648
2.4	139	142.2747	133.6843	151.9997	174.1472	129.1026	193.0881
2.5	139	142.8642	134.2739	152.6804	174.6858	129.7468	193.3042
2.6	141	143.4306	134.8403	153.3345	175.2032	130.3656	193.5136
2.7	143	143.9757	135.3853	153.9639	175.7011	130.9612	193.7168
2.8	142	144.5009	135.9105	154.5704	176.1809	131.5350	193.9142
2.9	148	145.0077	136.4173	155.1556	177.0911	132.0887	194.1060
3.0	150	145.9708	136.9069	155.7210	176.6439	132.6237	194.2927
3.1	153	146.4293	137.3804	156.2678	177.5237	133.1411	194.4745
3.2	158	146.8737	137.8389	156.7973	177.9426	133.6421	194.6517
3.3	161	147.3048	138.2833	157.3105	178.3485	134.1276	194.8246
3.4	163	147.7235	138.7144	157.8083	178.7424	134.5987	194.9933
3.5	160	148.1303	139.1331	158.2918	179.1248	135.0561	195.1581
3.6	169	148.5260	139.5399	158.7616	179.4965	135.5006	195.3192
3.7	164	148.9111	139.9356	159.2185	179.8580	135.9329	195.4768
3.8	169	149.2862	140.3207	159.6632	180.2098	136.3537	195.6309
3.9	173	149.2862	140.6959	160.0964	180.5525	136.7636	195.7819
4.0	173	149.6519	141.0615	160.5187	180.8865	137.1631	195.9297

TABLE A.5: Comparison of estimated values of pathloss models with field Measurements from BTS2 located in Korang town.

Distance(Km)	Measured Pathloss(dB)	Hata-Okumura (dB)	COST-231 (dB)	Lognormal (dB)	Ericson(dB)	SUI (dB)	ECC-33 (dB)
0.1	113	96.3784	87.7880	93.3222	132.2194	78.9549	203.1214
0.2	125	106.3886	97.7982	106.5344	141.3640	89.8924	203.1051
0.3	127	112.2442	103.6538	114.2631	146.7133	96.2903	204.5733
0.4	119	116.3988	107.8084	119.7466	150.5087	100.8298	206.2766
0.5	127	119.6213	111.0309	124.0000	153.4526	104.3509	207.9760
0.6	133	122.2543	113.6640	127.4753	155.8579	107.2278	209.6097
0.7	135	124.4805	115.8901	130.4136	157.8916	109.6602	211.1631
0.8	135	126.4089	117.8186	132.9588	159.6533	111.7672	212.6361
0.9	127	128.1099	119.5195	135.2039	161.2072	113.6258	214.0336
1.0	133	129.6315	121.0411	137.2122	162.5972	115.2883	215.3618
1.1	139	131.0079	122.4176	139.0289	163.8546	116.7922	216.6266
1.2	125	132.2645	123.6741	140.6875	165.0026	118.1652	217.8340
1.3	135	133.4205	124.8301	142.2132	166.0586	119.4282	218.9891
1.4	140	134.4907	125.9003	143.6258	167.0363	120.5976	220.0964
1.5	137	135.4871	126.8967	144.9409	167.9465	121.6863	221.1600
1.6	146	136.4191	127.8287	146.1710	168.7979	122.7046	222.1835
1.7	158	137.2946	128.7043	147.3266	169.5978	123.6613	223.1702
1.8	154	138.1201	129.5297	148.4161	170.3518	124.5632	224.1228
1.9	160	138.9009	130.3105	149.4467	171.0652	125.4163	225.0438
2.0	163	139.6417	131.0513	150.4244	171.7419	126.2257	225.9354

TABLE A.6: Comparison of estimated values of pathloss models with field measurements from BTS3 located in Soan garden.

Distance(km)	Measured Pathloss(dB)	Hata-Okumura (dB)	COST-231 (dB)	Lognormal (dB)	Ericson(dB)	SUI (dB)	ECC-33 (dB)
0.1	121	96.3784	87.7880	118.3222	132.2194	78.9549	272.2964
0.2	121	106.3886	97.7982	131.5344	141.3640	89.8924	272.2801
0.3	117	112.2442	103.6538	139.2631	146.7133	96.2903	273.7483
0.4	101	116.3988	107.8084	144.7466	150.5087	100.8298	275.4516
0.5	115	119.6213	111.0309	149.0000	153.4526	104.3509	277.1510
0.6	119	122.2543	113.6640	152.4753	155.8579	107.2278	278.7847
0.7	117	124.4805	115.8901	155.4136	157.8916	109.6602	280.3381
0.8	113	126.4089	117.8186	157.9588	159.6533	111.7672	281.8111
0.9	123	128.1099	119.5195	160.2039	161.2072	113.6258	283.2086
1.0	135	129.6315	121.0411	162.2122	162.5972	115.2883	284.5367
1.1	143	131.0079	122.4176	164.0289	163.8546	116.7922	285.8016
1.2	152	132.2645	123.6741	165.6875	165.0026	118.1652	287.0090
1.3	153	133.4205	124.8301	167.2132	166.0586	119.4282	288.1640
1.4	160	134.4907	125.9003	168.6258	167.0363	120.5976	289.2713
1.5	163	135.4871	126.8967	169.9409	167.9465	121.6863	290.3350
1.6	159	136.4191	127.8287	171.1710	168.7979	122.7046	291.3585
1.7	164	137.2946	128.7043	172.3266	169.5978	123.6613	292.3452
1.8	159	138.1201	129.5297	173.4161	170.3518	124.5632	293.2977
1.9	169	138.9009	130.3105	174.4467	171.0652	125.4163	294.2187
2.0	167	139.6417	131.0513	175.4244	171.7419	126.2257	295.1104

Appendix B

Distribution of Field Measurements at various Distances

The measurement data was checked for its fitting using the MATLAB. In this regard, the probability density functions (PDFs) of lognormal distribution are plotted at distances of 1000 m, 1500 m, 2000 m, 2500 m, 3000 m, 3500 m, 4000 m as shown in Fig B.1 to B.8. The curves of the PDFs corresponding to the lognormal distribution generated by using the distribution fitting tool in MATLAB.

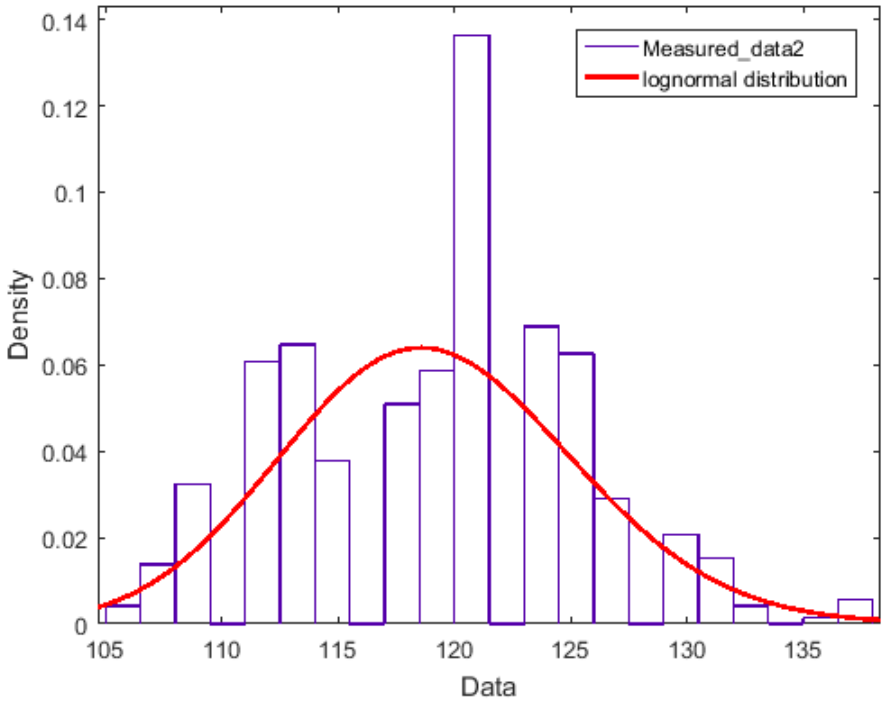

FIGURE B.1: Distribution of measured data at distance of 500m.

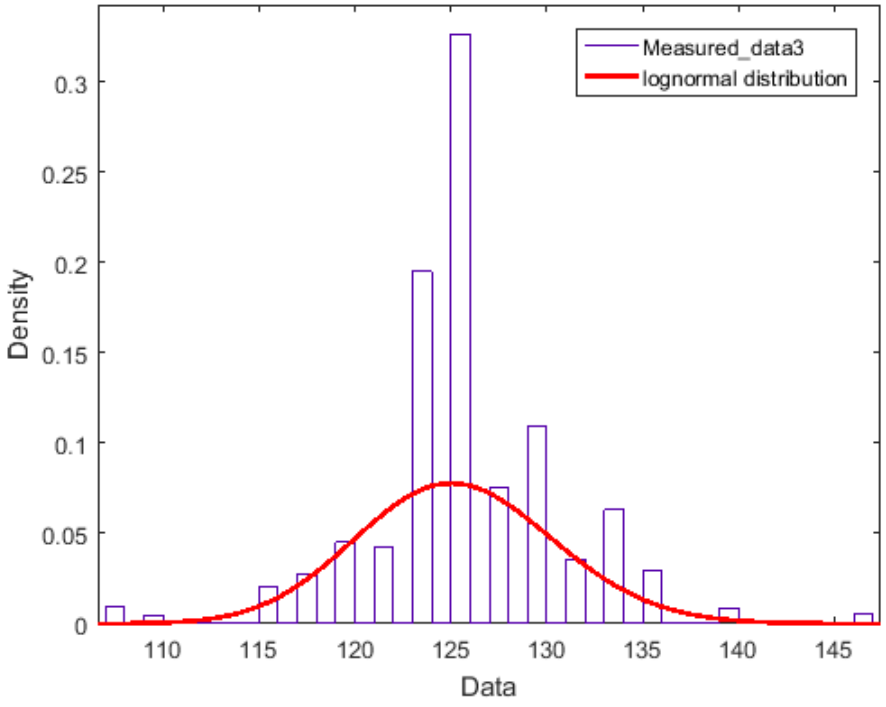

FIGURE B.2: Distribution of measured data at distance of 1000m.

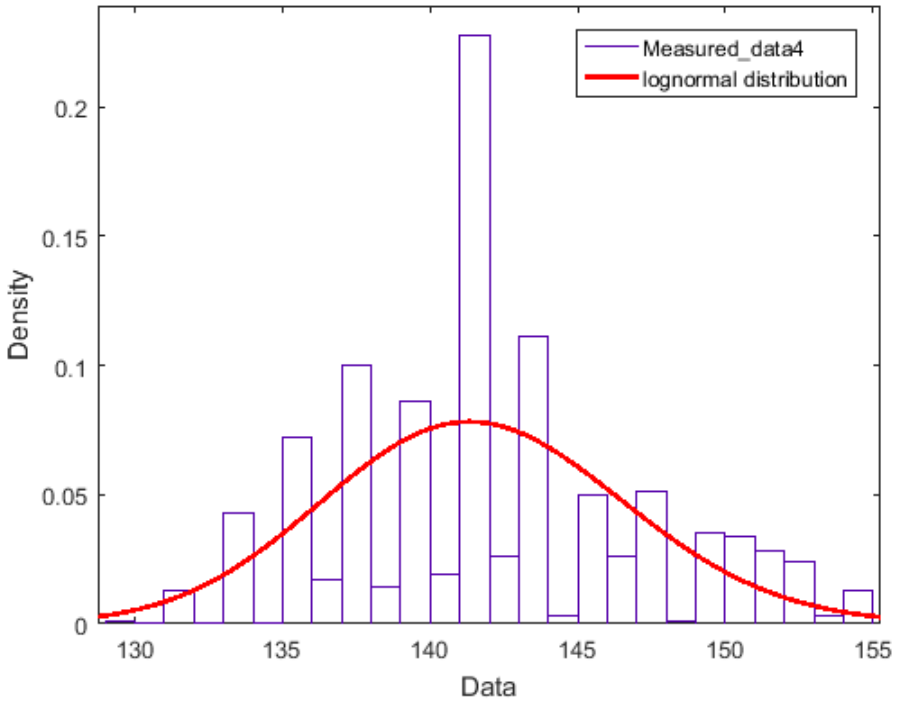

FIGURE B.3: Distribution of measured data at distance of 1500m.

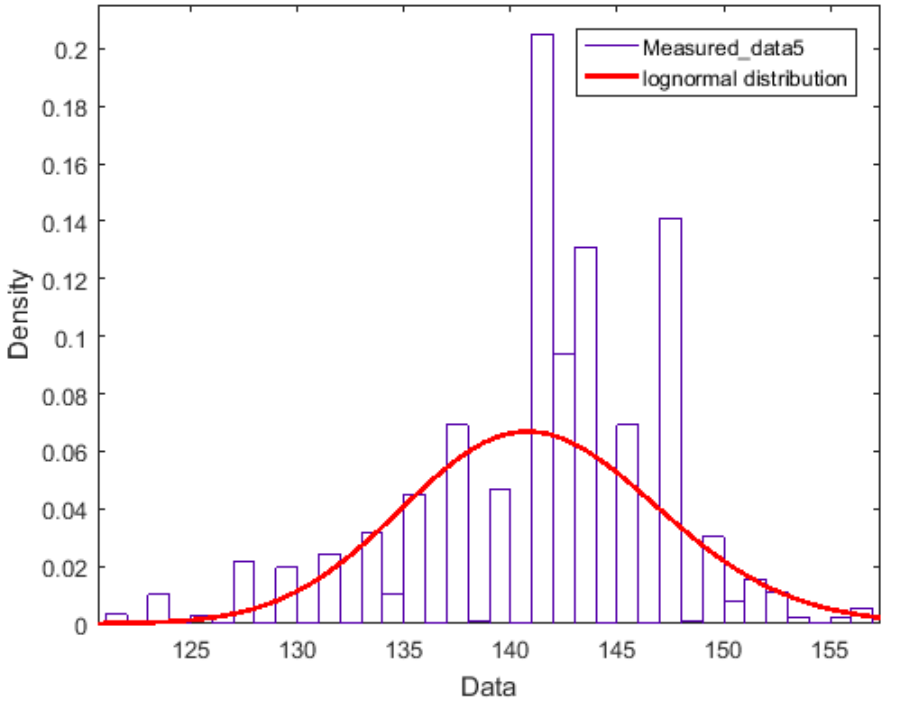

FIGURE B.4: Distribution of measured data at distance of 2000m.

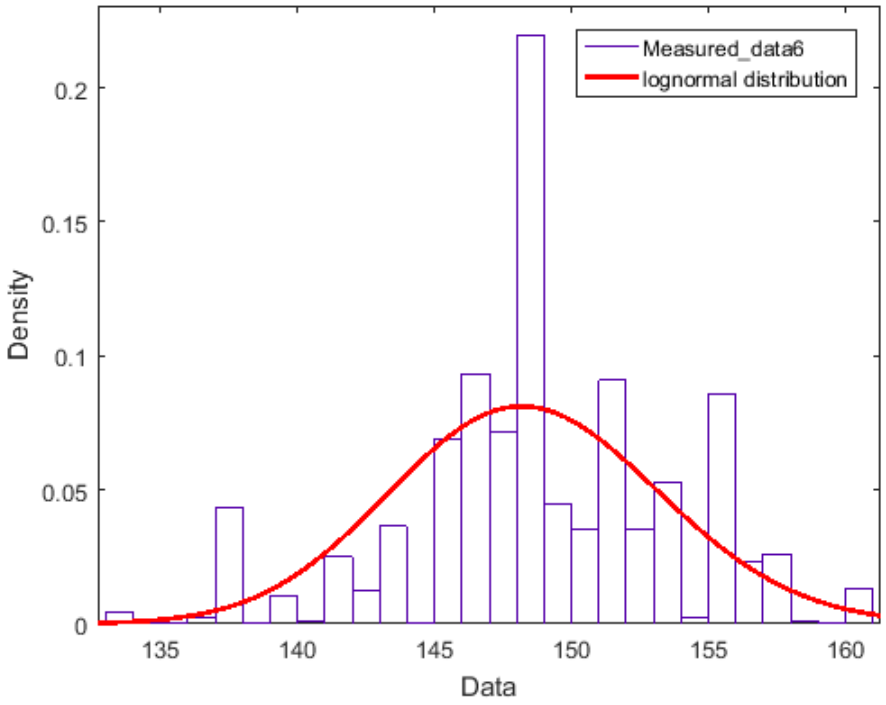

FIGURE B.5: Distribution of measured data at distance of 2500m.

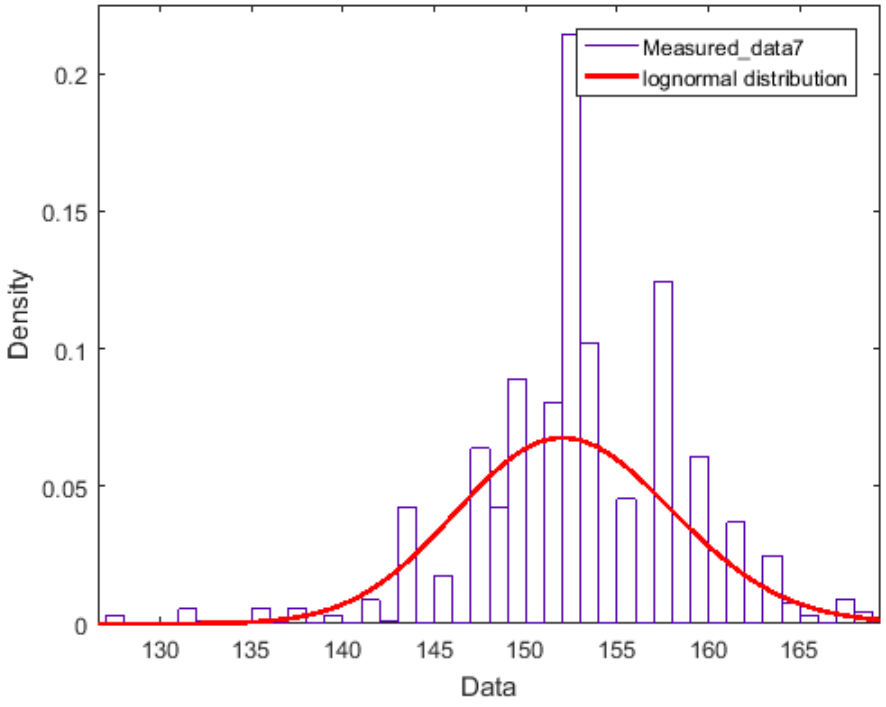

FIGURE B.6: Distribution of measured data at distance of 3000m.

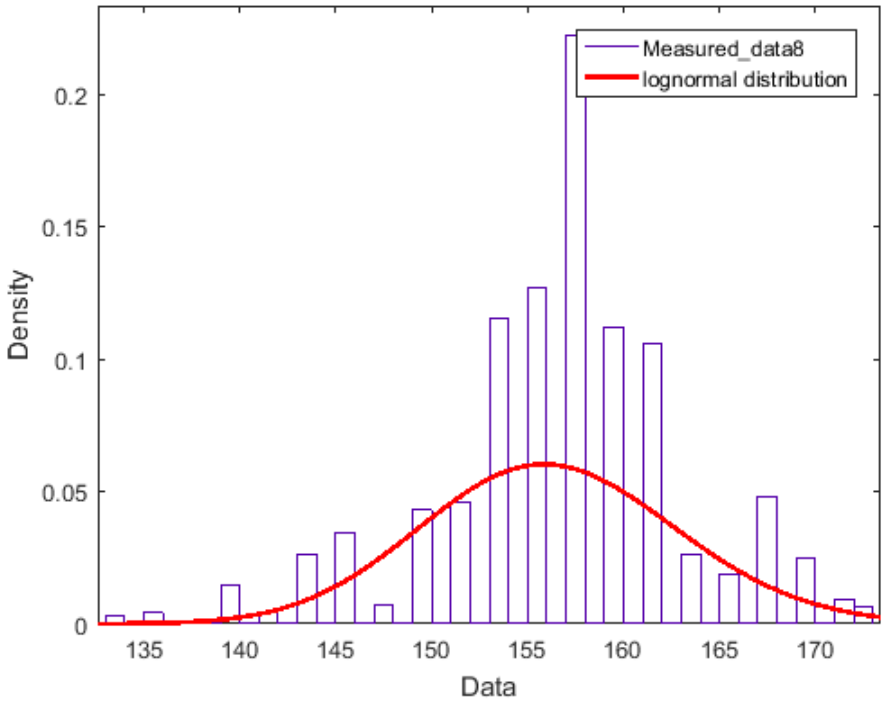

FIGURE B.7: Distribution of measured data at distance of 3500m.

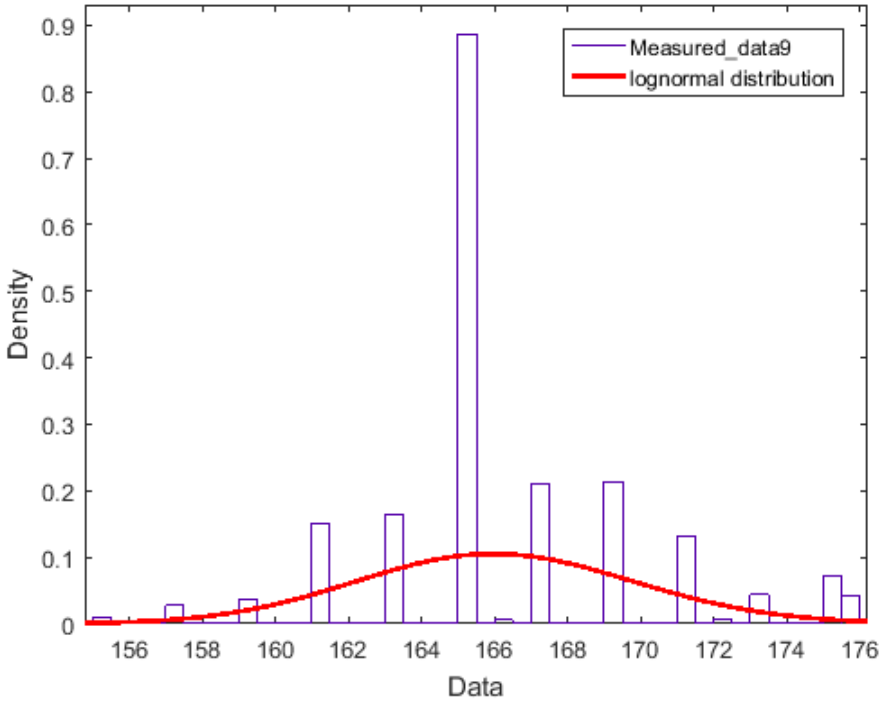

FIGURE B.8: Distribution of measured data at distance of 4000m.

Bibliography

[1] V. Erceg and L. Greenstein, "An empirically based path loss model for wireless channels in urban environments," *IEEE J. on Sel. Areas of Commun.*, vol. 17, no. 7, pp. 1205–1211, 1999.

[2] David, E. Dahlman, A. Furusk, Y. Jading, M. Lindstr, and S. Parkvall, "LTE: the evolution of mobile broadband," *IEEE Commun. mag.*, vol. 47, no. 4, pp. 44–51, 2009.

[3] B. Karakaya and A. Arslan, "An adaptive channel interpolator based on kalman filter for LTE uplink in high doppler spread environments," *EURASIP J. on Wireless Commun. and Netw.*, vol. 9, no. 1, p. 89751, 2009.

[4] G. S. Bola and G. S. Saini, "Path loss measurement and estimation using different empirical models for WiMAX in urban area," *Int. J. of Sci. and Eng. Res.*, vol. 4, no. 5, p. 1421–1428, 2013.

[5] S. Sharma, K. Purnima, "Comparative analysis of propagation path loss models with field measured data," *Int. J. of Eng. Sci. and Technol.*, vol. 2, no. 6, p. 2008–2013, 2010.

[6] L. H. Garah, M. Djouane, "Path loss models optimization for mobile communication in different areas," *Indonesian J. of Elect. Eng. and Comput. Sci.*, vol. 3, no. 1, p. 126–35, 2016.

[7] S. J. Song, Lingyang, *"Evolved cellular network planning and optimization for UMTS and LTE*," Boca Raton, CRC press, 2010.

[8] K. Crane, *"Propagation handbook for wireless communication system design,"* Boca Raton London, CRC press, 2003.

[9] M. Shahajahan, "Analysis of propagation models for WiMAX at 3.5 GHz," *Sign. Process. Telecommun.*, vol. 54, no. 2, pp. 307–308, 2009.

[10] T. S. Rappaport, *"Propagation handbook for wireless communication system design,"*. 2nd ed. IEEE Press Prentic Hall PTR,London Newyork,2005.

[11] M. Dottling, A. Jahn, and W. Wiesbeck, "A comparison and verification of 2D and 3D ray tracing propagation models for land mobile satellite communication," *IEEE Ant. and Propag. Soc. Int. Symp.*, vol. 1, IEEE, pp. 434–437, 2000.

[12] V. Erceg, L. J. Greenstein, S. Y. Tjandra, S. R. Parkoff, A. Gupta, B. Kulic, A. A. Julius, and R. Bianchi, "An empirically based path loss model for wireless channels in suburban environments,*IEEE J. on sel. areas in commun.*, vol. 17, no. 7, pp. 1205–1211, 1999.

[13] M. S. . M. A. R. M. A. Masud, "Bit error rate performance analysis on modulation techniques of wideband code division multiple access," *J. of Telecommun.*, vol. 10, no. 2, pp. 22–29, 2010.

[14] C. R. W. T. Ghassemzadeh S.S., R. Jana and V. Tarokh, "*A statistical path loss model for in-home UWB channels ultra wideband systems and technology,*" vol. 3, no. 1. IEEE, pp. 59–64, 2002.

[15] M. Hata, "Empirical formula for propagation loss in land mobile radio services," *IEEE trans. on Veh. Technol.*, vol. 29, no. 3, pp. 317–325, 1980.

[16] V. Abhayawardhana, I. Wassell, D. Crosby, M. Sellars, and M. Brown, "Comparison of empirical propagation path loss models for fixed wireless access systems," *IEEE 61st Veh. Technol. Conf.*, vol. 1, 2005, pp. 73–77.

[17] A. Mousa, Y. Dama, M. Najjar, and B. Alsayeh, "Optimizing outdoor propagation model based on measurements for multiple RF cell," *Int. J. of Comput. Appl.*, vol. 60, no. 5, 2012.

[18] S. Hamani and M. Oussalah, "Mobile location system using netmonitor and mappoint server, " in *Proc. of 6th Ann. Symp. on the Converg. of Telecommun. Netw. and Broadcast.*, Citeseer, 2006, pp. 17–22.

[19] Y. Okumura, "Field strength and its variability in VHF and UHF land-mobile radio service," *Rev. Electr. Commun. Lab.*, vol. 16, no. 8, pp. 825–873, 1968.

[20] R. S. Hassan, T. Rahman, and A. Abdulrahman, "LTE coverage network planning and comparison with different propagation models," *Telkomnika*, vol. 12, no. 1, p. 153, 2014.

[21] J. Milanovic, S. Rimac-Drlje, and K. Bejuk, "Comparison of propagation models accuracy for WiMAX on 3.5 GHz," *14th IEEE Int. Conf. on Elect., Circuits and Syst.*, IEEE, 2007, pp. 111–114.

[22] M. R. I. J. Chebil, A. K. Lwas and A. Zyoud, "Comparison of empirical propagation path loss models for mobile communication in the suburban area of kuala lumpur," *4th Int. Conf. on Mechatro.*, vol. 30, no. 04, pp. 1–5, 2011.

[23] W. Joseph and L. Martens, "Performance evaluation of broadband fixed wireless system based on IEEE 802.16," *IEEE Wireless Commun. and Netw Conf.*, vol. 2, 2006, pp. 978–983.

[24] Z. Sarkar, K.Tapan, K. Kim, A. Medouri, and M. Salazar-Palma, "A survey of various propagation models for mobile commun.," *J. of IEEE Antennas and Propag. Mag.*, vol. 45, no. 3, p. 51—82, 2003.

[25] H. R. Anderson, *"Fixed broadband wireless system design,"* John Wiley & Sons, 2003.

[26] N. A. Okumbor and R. Okonkwo Obikwelu, "Characterization of signal attenuation using pathloss exponent in south-south nigeria," *Int. J. of Emerg. Trends and Technol. in Comput. Sci.*, vol. 3, no. 3, p. 100—114, 2014.

[27] V. Kamboj, D. Gupta, and N. Birla, "Comparison of path loss models for WiMAX in rural environment at 3. 5 GHz," *Int. J. of Eng. Sci. and Technol. (IJEST)*, vol. 3, no. 2, pp. 1432–7, 2011.

[28] B. J. Cavalcanti, G. A. Cavalcante, M. T. Santos, G. M. Cantanhede, A. G. D'Assuncão, and L. M. de Mendonça, "Propagation models tuning for long term evolution and long term evolution-advanced using genetic algorithms and least mean square," pp. 1–6, 2018.

[29] M. Mollel MS, "Comparison of empirical propagation path loss models for mobile commun.," *Comput. Eng. and Intell. Syst.*, vol. 5, no. 9, pp. 1–0, 2014.

[30] M. S. Mollel and M. Kisangiri, "An overview of various propagation model for mobile commun.," *Sci., Comput. and Telecommun. (PACT) Pan Afri. Conf.*, vol. 206, no. 10, pp. 148–153, 2014.

[31] Anna Foerster, Alexander Foerster, *Emerging communications for wireless sensor networks*, 2011.

[32] M. Golestanian and C. Poellabauer, "Variloc: Path loss exponent estimation and localization using multi-range beaconing," *IEEE Commun. Lett.*, vol. 23, no. 4, pp. 724–727, 2019.

[33] G. Wang, H. Chen, Y. Li, and M. Jin, "On received-signal-strength based localization with unknown transmit power and path loss exponent," *IEEE Wireless Commun. Lett.*, vol. 1, no. 5, pp. 536–539, 2012.

[34] N. Salman, A. H. Kemp, and M. Ghogho, "Low complexity joint estimation of location and path-loss exponent," *IEEE Wireless Commun. Lett.*, vol. 1, no. 4, pp. 364–367, 2012.

[35] I. Guvenc, S. Gezici, and Z. Sahinoglu, "Fundamental limits and improved algorithms for linear least-squares wireless position estimation," *Wireless Commun. and Mob. Comput.*, vol. 12, no. 12, pp. 1037–1052, 2012.

[36] J. S. Seybold, *Introduction to RF propagation*, John Wiley and Sons, 2005.

[37] D. Hawbaker and T. Rappaport, "Indoor wideband radiowave propagation measurements at 1.3 GHz and 4.0 GHz," *Elect. Lett.*, vol. 26, no. 21, pp. 1800–1802, 1990.

[38] K. Ayyappan and P. Dananjayan, "Propagation model for highway in mobile communication systems," *Ubiquitous Comput. and Commun. J.*, vol. 3, no. 4, pp. 61–66, 2008.

[39] M. Versaci, S. Calcagno, F. La Foresta, and B. Cammaroto, "Path loss prediction using fuzzy inference system and ellipsoidal rules," *Amer. J. of Appl. Sci.*, vol. 9, no. 12, p. 1940, 2012.

[40] H. Ding, Z. Xu, and B. M. Sadler, "A path loss model for non-line-of-sight ultraviolet multiple scattering channels," *EURASIP J. on Wireless Commun. and Netw.*, vol. 2010, no. 1, p. 598572, 2010.

[41] Y. Singh, "Comparison of okumura, hata and COST-231 models on the basis of path loss and signal strength," *Int. J. of Comput. Appl.*, vol. 59, no. 11, 2012.

[42] K. G. Tan and T. A. Rahman, "Receiving antenna height dependence of radio propagation path loss in fixed wireless access environment," *Asia Pacific Microw. Conf. Microw. Enter the 21st Cent. Conf. Proc.*, vol. 3, IEEE, 1999, pp. 797–800.

[43] V. Gupta, S. Sharma, and M. Bansal, "Fringe area path loss correction factor for wireless communication," *Int. J. of Recent Trends in Eng.*, vol. 1, no. 2, p. 30, 2009.

[44] J. Chebil, A. K. Lawas, and M. Islam, "Comparison between measured and predicted path loss for mobile communication in malaysia," *World Appl. Sci. J.*, vol. 21, no. 6, pp. 123–128, 2013.

[45] P. Akinyemi, S. Azi, J. Ojo, and C. Abiodun, "Evaluation for suitable propagation model to mobile communications in south-south nigeria urban-terrain," *Am. J. Eng. Res.*, vol. 4, pp. 01–05, 2015.

[46] J.-M. Dricot and P. De Doncker, "High-accuracy physical layer model for wireless network simulations in ns-2," in *Int. Workshop on Wireless Ad-Hoc Netw.*,IEEE, 2004, pp. 249–253.

[47] G. Acosta-Marum and M. A. Ingram, "Six time-and frequency-selective empirical channel models for veh. wireless LANs," *IEEE Veh. Technol. Mag.*, vol. 2, no. 4, pp. 4–11, 2007.

[48] R. V. Akhpashev and A. V. Andreev, "COST-231 HATA adaptation model for urban conditions in LTE networks," *17th Int. Conf. of Young Specialists on Micro/Nanotechnologies and Elect. Devices (EDM)*, IEEE, 2016, pp. 64–66.

[49] P. K. Sharma and R. Singh, "Comparative analysis of propagation path loss models with field measured data," *Int. J. of Eng. Sci. and Technol.*, vol. 2, no. 6, pp. 2008–2013, 2010.

[50] R. Desimone, B. M. Brito, and J. Baston, "Model of indoor signal propagation using log-normal shadowing," *Long Island Syst., Appl. and Technol.*. IEEE, 2015, pp. 1–4.

[51] C. C. Pu, S. Y. Lim, and P. C. Ooi, "Measurement arrangement for the estimation of path loss exponent in wireless sensor network," *7th Int. Conf. on Comput. and Converg. Technol. (ICCCT)*, IEEE, 2012, pp. 807–812.

[52] M. Golestanian, J. Siva, C. Poellabauer, J. Ortiz, and A. de la Cruz, "Radio frequency-based indoor localization in ad-hoc networks," *Ad Hoc Netw.*, 2017.

[53] L. Klozar, J. Prokopec, S. Hanus, M. Slanina, and Z. Fedra, "Indoor channel modeling based on experience with outdoor urban measurement—multislope modeling," *IEEE Int. Conf. on Microw, Commun., Antennas and Elect. Sys.*,IEEE, 2011, pp. 1–4.

[54] K.-W. Cheung, J.-M. Sau, and R. D. Murch, "A new empirical model for indoor propagation prediction," *IEEE trans. on Veh. Technol.*, vol. 47, no. 3, pp. 996–1001, 1998.

[55] S. Y. Seidel and T. S. Rappaport, "914 MHz path loss prediction models for indoor wireless commun. in multifloored buildings," *IEEE trans. on Antennas and Propag.*, vol. 40, no. 2, pp. 207–217, 1992.

[56] Munir, Hamnah and Hassan, Syed Ali and Pervaiz, Haris and Ni, Qiang and Musavian, Leila, "Resource optimization in multi-tier HetNets exploiting multi-slope path loss model, "*IEEE Access*, vol. 5, pp. 8714–8726,2017. 2017.

[57] Zhang, Xinchen and Andrews, G. Jeffrey, "Downlink cellular network analysis with multi-slope path loss models, "*IEEE Trans. on Commun.*, vol. 63,no. 5, pp. 1881–1894,2015.

[58] Andrews, G. Jeffrey and Zhang, Xinchen and Durgin, D. Gregory and Gupta, K. Abhishek, "Are we approaching the fundamental limits of wireless network densification?, "*IEEE Commun. Mag.*, vol. 54,no. 10, pp. 184–190,2016.

[59] Romanous, Bashar and Bitar, Naim and Imran, Ali and Refai, Hazem, "Network densification: Challenges and opportunities in enabling 5G," *2015 IEEE 20th Int. Workshop on Comput. Aid. Model. and Des. of Commun. Links and Netw.*,IEEE, 2015, pp. 129–134.

[60] Liu, Junyu and Sheng, Min and Liu, Lei and Li, Jiandong, "Effect of densification on cellular network performance with bounded pathloss model, "*IEEE Commun. Lett.*, vol. 21,no. 2, pp. 346–349,2016.

[61] C. B. Andrade and R. P. F. Hoefel, "Network densification: Challenges and opportunities in enabling 5G," *Proc. 23rd Can. Conf. IEEE Conf. Elect. Comput. Eng.* ,2016, pp. 1–6.

[62] Wikipedia contributors, " G-NetTrack for 2G-3G-4G GSM-UMTS-LTE Monitoring and Test," Available: http://www.telecomhall.com/g-nettrack-and-other-great-tools-for-2g-3g-4g-gsm-umts-lte-monitoring-and-test.aspx, 2016, [Online; accessed 5-November-2019].

[63] Wikipedia contributors,"Cell Towers Map, Cellular Coverage, and Frequency Calculator," Available: https://www.cellmapper.net/Index, 2019, [Online; accessed 5-November-2019].